REVISTA MEXICANA DE CIENCIAS GEOLÓGICAS

Revista Mexicana de Ciencias Geológicas, v. 43, num. 2, August 2026, 140–160
ISSN-L 2007-2902
https://rmcg.unam.mx

Type: Original research

DIAMOND OPEN ACCESS

Xenarthrans from Sistema Calera Cave, Mexico, and radiocarbon and stable isotope analyses of the cave fauna

H. Gregory McDonald[1, a], Mário A.T. Dantas[2, b], Ramón Espinasa-Pereña[3] and Luis Espinasa[4, c, *]

[1] *3309 Snowbrush Court, Fort Collins, CO 80521, USA.*
[2] *Laboratório de Ecologia & Geociências, Universidade Federal da Bahia (IMS/CAT), Rua Hormindo Barros, 58, Bairro Candeias, CEP: 45.029-094, Vitória da Conquista, Bahia, Brazil.*
[3] *Sociedad Mexicana de Exploraciones Subterráneas, Ingenieros No. 29, Col. Escandón, Alcaldía Miguel Hidalgo. 11800, Mexico City, Mexico.*
[4] *School of Science, Marist University, 3399 North Rd, Poughkeepsie, New York, USA.*

* *Corresponding author (L. Espinasa) luis.espinasa@marist.edu*
[a] *0000-0001-6916-7237;* [b] *0000-0002-9141-1643;* [c] *0000-0002-2234-0407*

How to cite:
McDonald, H. G., Dantas, M. A. T. Espinasa-Pereña, R., & Espinasa, L. (2026). Xenarthrans from Sistema Calera Cave, Mexico, and Radiocarbon and Stable Isotope Analyses of the cave fauna. *Revista Mexicana de Ciencias Geológicas*, *43*(2), 140–160. DOI: https://dx.doi.org/10.22201/igc.20072902e.2026.2.1926

Manuscript received: February 22, 2026
Corrected manuscript received: May 19, 2026
Manuscript accepted: May 22, 2026
Published online: August 1, 2026

ABSTRACT

Recent investigations at Sistema Calera Cave (21°53'49"N, 98°55'52"W, 103 m a.s.l.), located in the Sierra de El Abra, San Luis Potosí, northeastern Mexico, have established the site as one of exceptional paleontological importance due to its remarkably diverse assemblage of fossilized vertebrate remains. Given the underwater depositional context, which likely contributed to collagen degradation, radiocarbon dating was performed on bioapatite, with results converted to collagen-equivalent values and calibrated to calendar years. Radiocarbon dates place specimens of *Bison* sp. (8423–8549 cal yr BP), *Tremarctos* cf. *floridanus* (12686–12752 cal yr BP), *Glyptotherium cylindricum* (12986–13166 cal yr BP), *Canis dirus* (13574–13666 cal yr BP), *Mammuthus columbi* (13729–13887 cal yr BP), *Eremotherium laurillardi* (23784–24065 cal yr BP), and *Smilodon fatalis* (31027–31178 cal yr BP) within the Late Rancholabrean. The range of dates indicates the assemblage represents a time-averaged fauna. The carbon isotopic signature ($\delta^{13}C$) suggests three main types of vegetation animals fed on: low-density forests, an arboreal savanna, and an ecotone between arboreal savanna to open savanna. Of 775 cataloged specimens, 37 are assigned to Xenarthra, including three sloth genera (*Eremotherium*, *Nothrotheriops*, and a megalonychid cf. *Nohochichak*) and one glyptodont (*Glyptotherium*). The co-occurrence of *Nothrotheriops*, typically associated with arid environments, with *Eremotherium* and *Glyptotherium*, which are linked to tropical and mixed grassland habitats, presents an unusual ecological association. Potential explanations for this uncommon association are discussed.

Key words: fossil; megafauna; xenarthrans; cave; Pleistocene; Rancholabrean; radiocarbon dating; carbon isotopic signature; Mexico

RESUMEN

Investigaciones recientes en la cueva Sistema Calera, ubicada en la Sierra de El Abra, San Luis Potosí, en el noreste de México, han establecido el sitio como un lugar de importancia paleontológica excepcional debido a su notable diversidad de restos de vertebrados fosilizados. Dado el contexto deposicional subacuático, que probablemente contribuyó a la degradación del colágeno, se realizaron fechamientos por radiocarbono en bioapatita; los resultados fueron convertidos a valores equivalentes

DOI: https://dx.doi.org/10.22201/igc.20072902e.2026.2.1926

de colágeno y calibrados a años calendario. Los datos de radiocarbono sitúan especímenes de Bison sp. (8423–8549 años cal AP), Tremarctos cf. floridanus (12686–12752 años cal AP), Glyptotherium cylindricum (12986–13166 años cal AP), Canis dirus (13574–13666 cal yr BP), Mammuthus columbi (13729–13887 años cal AP) Eremotherium laurillardi (23784–24065 años cal AP) y Smilodon fatalis (31027–31178 cal yr BP) dentro del Rancholabreano tardío. La firma isotópica de carbono ($\delta^{13}C$) sugiere tres tipos principales de vegetación de la que se alimentaban los animales: bosques de baja densidad, una sabana arbolada y un ecotono entre la sabana arbolada y la sabana abierta. De los 775 especímenes catalogados, 37 se asignaron a Xenarthra, incluyendo tres géneros de perezosos (Eremotherium, Nothrotheriops y un megalónquido cf. Nohochichak) y un gliptodonte (Glyptotherium). La coexistencia de Nothrotheriops, típicamente asociado a ambientes áridos, junto con Eremotherium y Glyptotherium, relacionados con hábitats tropicales y de pastizales mixtos, representa una asociación ecológica inusual. Se discuten posibles explicaciones para esta asociación anómala.

Palabras clave: *fósil; megafauna; xenartros; cueva; Pleistoceno; Rancholabreano; datación por radiocarbono, firma isotópica del carbono; México*

INTRODUCTION

Cave-based Pleistocene fossil sites in Mexico remain relatively underrepresented in the scientific literature. For example, Ferrusquía-Villafranca *et al.*, *(*2017) and Bonilla Díaz (2018) documented only 27 localities yielding Rancholabrean-age faunas. The Rancholabrean is divided into two subintervals, RA1 from 250000 to 115000 years ago and RA2 from 115000 to 12000 years ago (Bell *et al.*, 2004). Most described cave faunas are from RA2. Interest in these subterranean contexts in Mexico has increased considerably with the reporting of new sites not only in the mountainous portions of the country (*e.g.* McDonald *et al.*, 2020) but also in the submerged caves in the southern tropical habitat of the Yucatan Peninsula (Schubert *et al.*, 2019). Ongoing interdisciplinary collaborations between speleologists and paleontologists are poised to expand the national record of cave-based Pleistocene faunas (McDonald *et al.*, 2020).

Recent investigations at Sistema Calera cave, situated within the Sierra de El Abra, San Luis Potosí State, in northeastern Mexico (21°53'49"N, 98°55'52"W, 103 m a.s.l.), have established the site as a locality of exceptional paleontological significance, owing to its remarkably diverse assemblage of fossilized vertebrate remains. Espinasa-Pereña *et al.* (2024) initially reported 109 cataloged specimens. Subsequently, Espinasa and Espinasa (2025) documented 775 fossils, of which 249 were left in the cave. These represent only a small fraction of the thousands of fossils left *in situ*. Most specimens are exceptionally well-preserved, exhibiting a characteristic coating of manganese oxide along with partial permineralization. The manganese oxide typically forms a continuous layer over bone surfaces, indicative of diagenesis occurring under prolonged water-saturated conditions post-deposition. In some cases, secondary calcite encrustations are also present.

Preliminary taxonomic assessments indicate that the most abundant remains belong to the order Perissodactyla, particularly the genus *Equus*. Other specimens included artiodactyls (bovids, cervids, camelids, and tayassuids), proboscideans (*Mammuthus* and gomphotheres), large carnivorans (felids, *Arctodus*, *Canis latrans* and *Canis dirus*), testudines and lagomorphs. Included in the collection are 37 specimens of Xenarthra.

Given its exceptional taxonomic diversity and remarkable state of preservation, Sistema Calera is among the most important cave-based Pleistocene megafaunal localities in northeastern Mexico. Ongoing research at the site promises to yield additional valuable insights into the paleoecology, biogeography, and environmental dynamics of the Sierra Madre Oriental and adjacent regions during the Late Pleistocene. This study aims to contribute to a more precise chronological framework for the faunal assemblage within the Rancholabrean through radiocarbon dating of selected specimens, while also offering a more detailed examination of the xenarthran remains recovered from Sistema Calera.

Geological setting and landform development

The Sierra de El Abra is dominated by carbonate rocks belonging to the El Abra Formation (also known as El Doctor), which accumulated during the mid-Cretaceous (Albian–Turonian) as part of an extensive rudist-dominated reef system surrounding the Valles–San Luis Potosí carbonate platform (Carrillo-Bravo, 1971). The abrupt eastern escarpment of the range corresponds to the former reef margin and is characterized by muddy rudist buildups interlayered with abundant bioclastic material and fine carbonate sediments. In contrast, the interior portions of the platform consist of back-reef deposits that include several carbonate facies, such as calcilutites and calcarenites containing miliolids and rudist biostromes, particularly of *Toucasia* (Bonet, 1952; Bonet, 1963). It is within these back-reef limestones that the Calera cave system developed (Figure 1).

Toward the end of the Cretaceous, carbonate sedimentation gradually gave way to clastic deposition, resulting in the accumulation of shale units of the Agua Nueva, San Felipe, and Méndez formations, which progressively buried the carbonate platform and reef structures.

During the early Paleocene, regional tectonic activity caused folding and uplift of the area. Although deformation was relatively mild, several small anticlinal ridges developed, trending roughly parallel to the mountain range. Following uplift, erosion preferentially removed the shale units, exposing the limestones to surface processes. Once exposed, these carbonates evolved into a rugged karst landscape, shaped by dissolution from mildly acidic groundwater migrating along fractures and bedding planes (Fish, 2004; Elliot 2018).

Karst development and hydrogeological context

In the vicinity of the Calera system, the Agua Nueva Formation is absent, and the Méndez Formation has been entirely removed by erosion. As surface streams flowed over San Felipe shales, they progressively eroded them, deepening their channels until they breached the underlying limestone bedrock.

Where shale units remain at the surface, runoff occurs primarily through surface channels due to their low permeability. In contrast, exposed limestone areas lack surface drainage, as water rapidly infiltrates through the epikarst into the subsurface. Underground stream capture takes place once erosion removes the overlying shale cover,

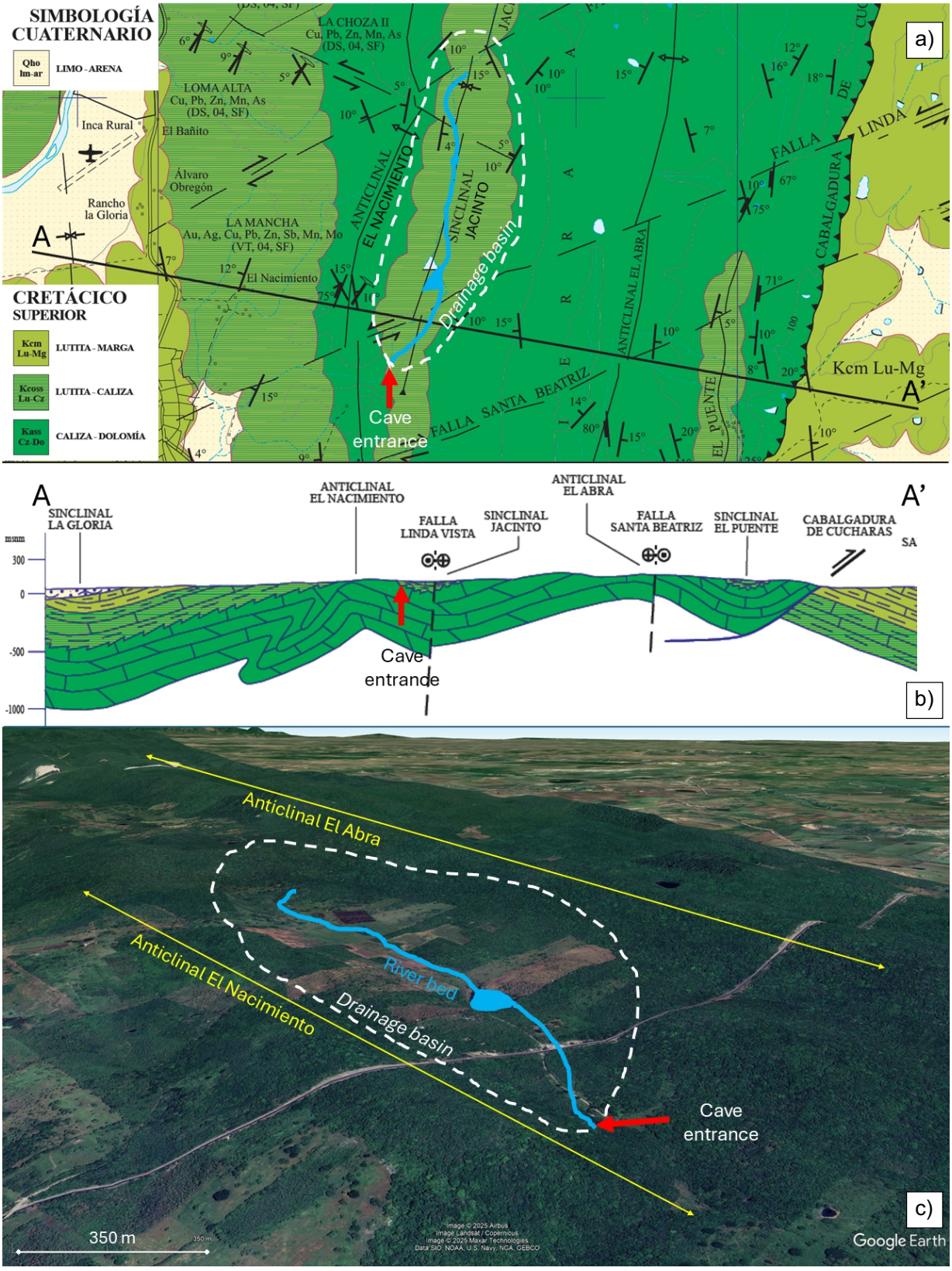

Figure 1. Hydrogeological context of the cave entrance (21° 53'49"N, 98° 55'52"W, 103 masl) of Sistema Calera Cave. a) The Sistema Calera Cave is formed through the capture of a small surface stream within the Jacinto synclinal valley, bordered by the El Nacimiento anticlinal ridge and the El Abra anticlinal ridge. b) Profile illustrating that the entrance of the cave is in the contact between shales (Lutita) and the limestone (Caliza). b) In the Jacinto synclinal drainage doline, water drains through the Calera cave system. a) and b) Modified from Servicio Geológico Mexicano (2008). c) Modified from Image © Google Earth / Maxar.

allowing surface waters to access the underlying El Abra limestones (Mitchell *et al.*, 1977). It is likely that limestone exposure initially occurred along elevated ridges, with modern sink points developing later in lower-lying areas. As a result, the northern entrances of the Calera cave system occur precisely at the boundary between the San Felipe shales and the underlying El Abra limestones (Figure 1a).

The Calera cave system, together with the nearby Sótano del Toro, formed through the capture of a small surface stream within the Jacinto synclinal valley, bordered by the El Nacimiento anticlinal ridge and the El Abra anticlinal ridge in the western margin of the southern Sierra de El Abra (Figure 1). The Jacinto synclinal has a drainage valley 3.3 km long and 1.8 km wide that forms a closed valley or doline, where water can only escape through the Calera cave system (Figure 1). A comprehensive description of the cave geomorphology, hydrology, and detailed cartography is provided in Espinasa-Pereña *et al.*, (2024).

Chronology of cave development and fossil deposition

A chronological framework for caves in the Sierra de El Abra was outlined by Espinasa and Espinasa (2015), who linked cave initiation to the timing of limestone exposure following erosion of overlying impermeable strata. Applying this approach to the Calera system, the elevation of the cave entrance (92 m above sea level) relative to the local base level (48 m above sea level) suggests that speleogenesis began sometime between approximately 1.17 and 0.29 million years ago (Espinasa & Espinasa 2015).

Independent support for a young age of the system comes from geomorphic criteria described by Mitchell *et al.* (1977), who noted that the relative age of stream sinks along the western flank of the Sierra de El Abra can be inferred from the degree of canyon incision and the morphology of the sink entrance. At Sótano del Toro, the ephemeral stream that enters the cave during periods of heavy rainfall has not produced a discernible canyon, and the margin of the doline coincides directly with the lithologic boundary between the San Felipe shales and the El Abra limestone. These features are consistent with a very recent episode of stream capture and align with the previously proposed age range.

Despite this youthful surface expression, the cave preserves evidence of multiple phases of internal development. An upper passage level, originally formed under phreatic conditions, was subsequently modified by vadose erosion and later abandoned as flow shifted to a lower active level. That lower level itself appears to be undergoing capture by an even deeper conduit, indicating at least one, and possibly two, episodes of water-table lowering since cave formation began (Espinasa-Pereña *et al.*, 2024). Vertebrate fossils occur throughout all passages that are subject to periodic flooding, regardless of whether they originated under phreatic or vadose conditions. This distribution implies that the main phase of fossil accumulation postdates the earlier stages of cave development and corresponds to the most recent erosional phase. Consequently, the fossils are substantially younger than the inferred onset of speleogenesis.

The cave is subject to periodic flooding, which has and continues to redistribute fossils throughout its passages resulting in a time-averaged sample. The spatial association of remains is governed less by stratigraphic age and more by hydraulic sorting, with bone transport and accumulation determined by their shape, weight and density within sediment embankments formed by high-energy flood events (Espinasa & Espinasa, 2025). Thus, stratigraphic dating for the deposition of fossils is not possible.

Based on geomorphic and speleogenetic indicators, the faunal assemblage was tentatively dated by Espinasa-Pereña *et al.*, (2024) to the late Rancholabrean (RA2, 115000 to 12000 years BP) based on biostratigraphically characteristic taxa.

This study aims to describe the Xenarthrans for Sistema Calera Cave and to give a more precise chronological framework for when the deposition of fossils occurred.

METHODS

Study material

Permits from the Instituto Nacional de Antropología e Historia (INAH) for the collecting and study of the material are 401.1S.3-2024/138 and 401.1S.3-2025/147. Permit No. 401.3S.16-2025/155 for exportation of material for radiocarbon dating was provided by INAH.

Samples were given field collection numbers and custodial collection numbers. Field collection numbers are S1-S117 for field season 2022-2023, R1-R245 for field season 2024, and U1-U237 for field season 2025. The custodial collection for the S samples is the Sociedad Mexicana de Exploraciones Subterráneas (SMES) and were given INAH numbers 3380PF 1-67. The custodial collection for the R and U samples is the Instituto de Geología, Universidad NAcional Autónoma de México (UNAM), and the samples kept in this collection that are described in this study were assigned numbers IGM 14640-14679.

For significant fossils found above water, iPhone cameras were used to document their position *in situ*. For those found underwater, the Qysea underwater drones, models Fifish V6 and V6s, were used. They are equipped with a 1/2.3" SONY CMOS sensor capable of capturing 12MP high-resolution images. The videos captured by these ROVs are in 4K resolution. With these photos and videos, 3D images can be visualized with the sketchfab.com program available via the internet. The locations of significant fossils were recorded on the map of the cave.

Field collection followed the methodology outlined by Jiménez Hidalgo *et al.*, *(*2024). As most specimens were situated on the sediment surface and only partially embedded, they could be easily recovered by surface collection. In submerged areas, fossils were collected using scuba equipment, supported by Qyasea underwater drones.

Excavation was minimal and limited primarily to fossil-bearing clay deposits located within sheltered rock alcoves. In these deposits, sediment was carefully dislodged either manually or with the assistance of a Dewalt 20V MAX cordless power cleaner. Sediment removed from these contexts was wet-sieved *in situ* to maximize fossil recovery. These deposits yielded exceptionally well-preserved specimens, including whole skulls, likely due to the protective microenvironment and fine-grained matrix (Figure 2).

In the "Glyptodont Pool", beneath the "Arrastre lodoso" (Espinasa-Pereña *et al.*, 2024, map in fig. 2k), the ceiling and floor converge resulting in the formation of a narrow alcove. Within this very narrow alcove there are clay deposits of a maximum thickness of about 0.5 meters. Embedded in this clay are some of the most abundant and best-preserved fossils. The cave environment for excavating this clay-filled alcove presented considerable logistical challenges. The narrow confines (ceiling height of <60 cm) and standing water—up to 40 cm deep—required collectors to lie flat, crawl forward until one cheek was submerged, with the nose barely above water and the head scraping against the ceiling (Figure 3).

Recovered fossils were individually stabilized for transport, labeled with a unique identification code, and sealed in plastic bags to prevent rapid desiccation. Specimens were then gently cleaned using tap water and a soft-bristled toothbrush to remove adhering clay. They were then air-dried gradually at room temperature in a shaded environment to minimize potential damage from sudden moisture loss.

Figure 2. Context in which some specimens were found. a) At the bottom of the Toro #2 pit, two large rock slabs formed cracks (white arrows) that became filled with clay and sediment. b) Use of a power cleaner to remove sediment revealed fossils embedded within the crack (blue arrow). c-d) One of the recovered specimens consisted of a partial skull of *Eremotherium. laurillardi*, exhibiting a well-preserved palate and the alveoli of two molariform teeth.

Once fully dried, all specimens were photographed using either an iPhone 12 mini or a Nikon Z9 camera equipped with a 105 mm macro lens. Lighting was provided by two SB-910 flashes synchronized via an SU-800 wireless transmitter. Image post-processing was performed using Adobe Lightroom. High-resolution copies of all photographs are available upon request by contacting the corresponding author.

Radiocarbon dating (^{14}C AMS)

Specimens used for radiocarbon dating are in Figure 4 and Table 1. The ^{14}C Accelerator Mass Spectrometry radiocarbon analyses and carbon stable isotope ratio δ^{13}C analyses were performed at the Center for Applied Isotope Studies at the University of Georgia. The crushed bone was treated with diluted 1N acetic acid to remove surface absorbed and secondary carbonates. Periodic evacuation ensured that evolved carbon dioxide was removed from the interior of the sample fragments, and fresh acid was allowed to reach the interior micro-surfaces. The chemically cleaned sample was then reacted under vacuum with 100 % phosphoric acid to dissolve the bone mineral and release carbon dioxide from the bioapatite. The resulting carbon dioxide was cryogenically purified from the other reaction products and catalytically converted to graphite using the method of Vogel *et al.*, (1984). Graphite ^{14}C/^{13}C ratios were measured using the CAIS 0.5 MeV accelerator mass spectrometer. The sample ratios were compared to the ratio measured from the Oxalic Acid I (NBS SRM 4990). The sample ^{13}C/^{12}C ratios were measured separately using a stable isotope ratio mass spectrometer and expressed as δ^{13}C with respect to Vienna Pee Dee Belemnite (V-PDB), with an error of less than 0.1 ‰. The quoted uncalibrated dates are in radiocarbon years before 1950 (years BP), using the Libby ^{14}C half-life of 5,568 ± 30 years. The error is quoted as one standard deviation and reflects both statistical and experimental errors. The date has been corrected for isotope fractionation.

Preliminary tests showed there was not sufficient collagen for dating because the material had been underwater, resulting in the degradation and loss of collagen. Consequently, we chose to perform radiocarbon dating for all samples (Table 1) using bioapatite ($^{14}C_{bioapatite}$) and converted it to collagen expected values ($^{14}C_{collagen}$) through the general regression (Equation 1) proposed by Dantas and Cherkinsky (2023) which used 28 samples, presents a strong correlation ($R^2 = 0.98$), lower values of the percent predicted error (%PE = 0.01), and standard error of the estimate (%SEE = 25). Subsequently, the age was calibrated to calendar years before the present, applying the same standard error identified in the $^{14}C_{bioapatite}$, using the CALIB 8.2 program (Reimer *et al.*, 2020), INTCal20 curve (Reimer *et al.*, 2013), and 2σ confidence intervals.

$$\mathrm{Log}_{10}{}^{14}C_{collagen} = 1.09^{*}\log_{10}{}^{14}C_{bioapatite} - 0.31 \qquad (1)$$

Stable isotope approach for dietary and habitat inference

Stable carbon (δ^{13}C) and oxygen (δ^{18}O) isotope analyses were performed on the hydroxyapatite of the structural carbonate of bone in all the samples. Although we are aware that bone is more susceptible to diagenesis, we tentatively compared the results of bone with the enamel.

Figure 3. Confined passageway of "Glyptodont Pool". a) The red arrow indicates the fossil-bearing clay layer. b) Power-washing the clay matrix to expose embedded fossils; a bovid horn core is partially exposed in the sediment (blue arrow). c-d) Recovery of a molariform tooth from the giant ground sloth *Eremotherium laurillardi* (white arrows), extracted from a narrow alcove where the cave ceiling and floor converge, encasing the specimen within the clay.

These analyses were performed at the Center for Applied Isotope Studies from the University of Georgia (Georgia, USA). All samples were cleaned using an ultrasonic bath with distilled water and allowed to dry naturally. They were then fragmented into smaller parts and treated with 1 M dilute acetic acid to remove absorbed superficial and secondary carbonates. Periodic evacuation ensured the removal of carbon dioxide from within the sample fragments, allowing fresh acid to reach even the interior microsurfaces. The chemically cleaned samples were then reacted under a vacuum with 100% phosphoric acid, dissolving the bone mineral and releasing carbon dioxide from the hydroxyapatite (Cherkinsky, 2009). All results are presented using delta notation: $\delta = [(R_{sample}/R_{standard} - 1)*1000]$ (Coplen, 1994). The reference for carbon isotope values ($R = {}^{13}C/{}^{12}C$) is V-PDB, while for oxygen values ($R = {}^{18}O/{}^{16}O$) is V-SMOW.

The results were interpreted based on $\delta^{13}C$ standards considering two types of resources, C_3 plants (resource 1, $\delta^{13}C_1 = -27 \pm 3$ ‰) and C_4 grasses (resource 2, $\delta^{13}C_2 = -13 \pm 2$ ‰) and the impacts of the Suess effect (2 ‰; Keeling *et al.*, 1979), where resource 1, designated as $\delta^{13}C_1$, represents C_3 plants utilizing a three-carbon fixation pathway that thrives in cool, wet environments and includes most trees, shrubs, and temperate crops, while resource 2, designated as C_2, represents C_4 grasses utilizing a four-carbon water-saving pathway adapted to hot, arid climates and including tropical grasses, maize, and sugarcane. Tejada-Lara *et al.* (2018) showed that hydroxyapatite (ε^*) enrichment in the body increases with body mass. The taxa studied presented an average body mass varying between 60 and 10000 kg (Christiansen & Harris, 2005; Anyonge & Roman, 2006; Carbot-Chanona *et al.*, 2022; Carlini *et al.*, 2022; Jiménez-Moreno *et al.*, 2022), with ε^* varying between 12.7 ‰ and 15.1 ‰. To avoid the use of different values of ε^*, we chose to use three classes of enrichment, 13 ‰ (*Canis dirus*, 60 kg, 12.7 ‰; *Smilodon fatalis*, 220 kg, 13.2 ‰), 14 ‰ (*Glyptotherium cyclindricum*, 375 kg, 13.5 ‰; *Bison* sp., 900 kg, 13.9 ‰; *Tremarctos* cf. *floridanus*, 950 kg, 13.9 ‰), and 15 ‰ (*Eremotherium laurillardi*, 4450 kg, 14.7 ‰; *Mammuthus columbi*, 10000 kg, 15.1 ‰), based on the estimated body mass of the studied taxa. CAM plants (*Crassulacean Acid Metabolism* plants fix carbon at night to conserve water in extremely arid environments, including cacti and pineapples) were not included, as their fruit dispersal is predominantly mediated by lizards (Godínez-Álvarez, 2004; Gomes *et al.*, 2014; 2016), birds (Bregman, 1988; Gomes *et al.*, 2014), and bats (Godínez-Álvarez & Valient-Banuet, 2000; Godínez-Álvarez *et al.*, 2002).

The proportions of food resources for herbivores and habitat use for omnivores and carnivores ($p_1 = C_3$ plants; $p_2 = C_4$ grasses) were estimated using the carbon isotope results of the studied taxa ($\delta^{13}C_{mix}$) following Equations 2 and 3 modified from Phillips (2012).

$$\delta^{13}C_{mix} = \delta^{13}C_1 p_1 + \delta^{13}C_2 p_2 \quad (2)$$

$$1 = p_1 + p_2 \quad (3)$$

Based on the proportion (p_i) of food resources, these taxa could be classified as grazers ($p_iC_4 > 85$ %), mixed-feeder "grazer" ($p_iC_4 > p_iC_3$), mixed-feeder "browser" ($p_iC_4 < p_iC_3$), and browser ($p_iC_3 > 85$ %), based on grazers from Africa (Bocherens *et al.*, 1996; Kingston & Harrison, 2007; Cerling & Harris, 1999; Cerling *et al.*, 2008).

The estimated potential of the herbivore and omnivore contribution to the isotopic signature of the dire wolf *Canis dirus* and saber tooth cat *Smilodon fatalis* were calculated through a mathematical mixing model using only the carbon isotope signatures. The proportions of food sources ($p_1, p_2, ..., p_n$) reflected by the isotopic composition of the sampled tissues were estimated using a one-isotope mathematical mixing model (Phillips, 2012). In these linear equations, three taxa that lived in the same time period (*Mammuthus columbi*; *Glyptotherium cyclindricum*; and *Tremarctos* cf. *floridanus*; Table 1)

Figure 4. Specimens used for radiocarbon dating. a) *Bison* sp. IGM 14675 (S108), metatarsal. b) *Tremarctos* cf. *floridanus* IGM 14676 (U199), skull. c) *Glyptotherium cyclindricum* IGM 14673 (U215), carapace osteoderm. d) *Canis dirus* IGM 14677 (R13), skull. e) *Mammuthus columbi* IGM 14678 (U197), molar. f) *Eremotherium laurillardi* IGM 14641 (U201), maxilla. g) *Smilodon fatalis* IGM 14679 (U36), lower jaw. All scales in cm.

were used as potential sources of food. We also added a mean value of -1.5 ‰ to the carbon isotopic signature of the carnivores, insectivores, and omnivores to correct for trophic fractionation (Fricke *et al*., 2007 and references therein). These data were utilized in Equation 4 in Excel (Microsoft Corporation, Redmond, Washington) and using the Solver supplement (assuming non-negative values):

$$\delta^{13}C_{mix} = \delta^{13}C_1 p_1 + \delta^{13}C_2 p_2 + \delta^{13}C_3 p_3 \quad (4)$$
$$1 = p_1 + p_2 + p_3$$

To estimate the mean and maximum potential prey size (*pps*) for *Canis dirus* at 12-13 ky, we used regressions (Equations 5 and 6) for canids proposed by Prevosti and Vizcaino (2006), where *bm* is the body mass (in kg) of the carnivore.

$$\mathrm{Log}_{10}pps_{mean} = 1.97^{*}\mathrm{Log}_{10}bm - 1.60 \ (R^2 = 0.56) \quad (5)$$
$$\mathrm{Log}_{10}pps_{max} = 1.88^{*}\mathrm{Log}_{10}bm - 0.40 \ (R^2 = 0.90) \quad (6)$$

Finally, considering the hydroxyapatite enrichment values used here (13–15 ‰), the enrichment associated with the Suess effect (2 ‰; Keeling *et al.*, 1979), and the expected $\delta^{13}C$ values for different habitats in the Americas (Domingo *et al.*, 2012), we interpreted the carbon isotopic signatures obtained from the analyzed material in terms of the habitats occupied by these taxa during the Late Pleistocene in northeastern Mexico. These habitats were classified as closed-canopy forests, low-density forests, arboreal savannas, arboreal-to-open savannas, and open savannas (Table 2).

RESULTS

Temporal range of the cave fossils

Radiocarbon dating of seven specimens (Figure 4) places the occurrence of these taxa in the late Rancholabrean, (RA2) between eight and 31 ka (Table 1). However, as discussed in more detail, the range of dates indicates that the fauna is a time-averaged sample, and not all taxa may have been contemporaries. The youngest date was from a bison *Bison* sp., with an age of 8423–8549 cal yr BP

Table 1. Taxa, material number, radiocarbon laboratory number, carbon isotopes signature ($\delta^{13}C$), body mass enrichment ($\mathcal{E}^{*}$), proportional contributions (p_i, %) of food sources, diet (mfG – mixed feeder "grazer", mfB – mixed feeder "browser", O – omnivore, C – carnivore), radiocarbon dates in bioapatite ($^{14}C_{bioapatite}$) converted to collagen ($^{14}C_{collagen}$), and calibrated ages (IntCal20 curve) for extinct Late Pleistocene megafauna from Sistema Calera cave. *Considering -1.5 % to correct trophic fraction.

Taxa	$\delta^{13}C$	$\mathcal{E}^{*}$	p_i (%)		Diet	$^{14}C_{bioapatite}$	$^{14}C_{collagen}$	Cal. Age
			C_3	C_4				
***Bison* sp.** Metatarsal IGM 14675 (S108), UGAMS 72925	-4.2	14.0	51	49	mfB	7100 ± 25	7725 ± 25	8423–8549
Tremarctos* cf. *floridanus Skull IGM 14676 (U199), UGAMS 75306	-11.4*	14.0	100	-	O	9600 ± 40	10732 ± 40	12686–12752
Glyptotherium cyclindricum Carapace osteoderm IGM 14673 (U215), UGAMS 75308	-4.7	14.0	55	45	mfB	9950 ± 40	11159 ± 40	12986–13166
Canis dirus Skull IGM 14677 (R13), UGAMS 77476	-7.0*	13.0	64	36	C	10440 ± 30	11759 ± 30	13574–13666
Mammuthus columbi Molar IGM 14678 (U197), UGAMS 75305	-6.7	15.0	76	24	mfB	10580 ± 60	11931 ± 60	13729–13887
Eremotherium laurillardi Maxilla IGM 14641 (U201), UGAMS 75307	-10.0	15.0	100	-	mfB	16910 ± 40	19892 ± 40	23784–24065
Smilodon fatalis Lower jaw IGM 14679 (U36), UGAMS 77477	-7.0*	13.0	64	36	C	22330 ± 50	26933 ± 50	31027–31178

($^{14}C_{bioapatite}$ = 7100±25 yr BP; $^{14}C_{collagen}$ = 7725±25 yr BP; Table 1). Four specimens from different taxa had similar ages between 12-13 cal yr BP: the dire wolf *Canis dirus* (13574-13666 cal yr BP; $^{14}C_{bioapatite}$ = 10440±30 yr BP; $^{14}C_{collagen}$ = 11759±30 yr BP; Table 1), the bear *Tremarctos* cf. *floridanus* (12686-12752 cal yr BP; $^{14}C_{bioapatite}$ = 9600±40 yr BP; $^{14}C_{collagen}$ = 10732±40 yr BP; Table 1), the glyptodont *Glyptotherium cyclindricum* (12986-13166 cal yr BP; $^{14}C_{bioapatite}$ = 9950±40 yr BP; $^{14}C_{collagen}$ = 11.159±40 yr BP; Table 1), and the mammoth *Mammuthus columbi* (13729-13887 cal yr BP; $^{14}C_{bioapatite}$ = 10580±60 yr BP; $^{14}C_{collagen}$ = 11931±60 yr BP; Table 1). The oldest specimens were an individual of the giant sloth *Eremotherium laurillardi* with an age of 23,784-24,065 cal yr BP ($^{14}C_{bioapatite}$ = 16910±40 yr BP; $^{14}C_{collagen}$ = 19892±40 yr BP; Table 1) and a specimen of the sabretooth cat *Smilodon fatalis* with an age of 31027-31178 cal yr BP ($^{14}C_{bioapatite}$ = 22330±50 yr BP; $^{14}C_{collagen}$ = 26933±50 yr BP; Table 1).

Xenarthran remains

To date, a total of 775 specimens have been documented from the Sistema Calera cave, of these, 249 remain *in situ*, while 526 have been extracted for detailed analysis. Among the recovered specimens, 37 have been identified as belonging to the order Xenarthra. Remains of ground sloths are the most abundant (n = 26), followed by the glyptodont (n = 11). Members of the Xenarthra are represented by three genera of sloths, *Eremotherium laurillardi*, *Nothrotheriops shastensis* and a megalonychid cf. *Nohochichak* and by one glyptodont, *Glyptotherium cyclindricum*.

Among the remains assigned to ground sloths, two are ungual phalanges (claws) from the third digit of the foot (Figure 5), three are isolated teeth (Figure 6), five are cranial fragments (Figure 7), ten are long bones (Figure 8), four are vertebrae (Figure 9), and two are elements of the pectoral or pelvic girdles. Of these, twenty-one have received tentative species recognition (see below). All eleven specimens attributed to glyptodonts consist exclusively of carapace osteoderms (Figure 10). Images of the *Eremotherium* claw can be seen in 3D at https://skfb.ly/oS8xv, https://skfb.ly/oSyGT, and https://skfb.ly/oSyGV. Image of the *Eremotherium* partial skull is at https://sketchfab.com/3d-models/giant-ground-sloth-skull-mexico-expedition-2025-fb6cc3989af34f41b91917e86ad0caee and the *Glyptotherium* osteoderms at https://sketchfab.com/3d-models/glyptadon-shell-baccc9bc68754e79bca522c9c2475797.

Systematics

Order Pilosa Flower, 1883
Suborder Folivora Delsuc *et al.*, 2001
Family Megatheriidae Gray, 1821
Genus *Eremotherium* Spillmann, 1948
Eremotherium laurillardi Lund, 1842

Material: Ungual phalange: IGM 14668 (R49) Figures 5a and 5c; Molar: IGM 14669 (U35) Figures 6c and 7a; Cranial fragments: IGM 14640-14644 (U191, U201, U206, U220 and U232) Figures 7a-7e, 7i; Proximal end of the left femur IGM 14650 (U186); Carpal? IGM 14651 (U187); Podial? IGM 14649 (U185).

The five cranial fragments were found by the side of the pool under the Toro #2 entrance (Espinasa and Espinasa 2025), inside a large crack between two slabs of rock covered by sediment (Figure 2).

Table 2. Isotopic habitat considering body mass enrichment (13-15 ‰) and Suess effect (2 ‰). Labels. CCF – closed-canopy forests, LDF – lower density forests/tree savanna, AS – arboreal savanna/savanna woodland, A-OS – arboreal to open savanna/shrub savanna, OS – open savanna/grass savanna.

ε* (‰)	CCF (‰)	LDF (‰)	AS (‰)	A-OS (‰)	OS (‰)
13	-21 to -15	-15 to -10	-10 to -7	-7 to -2	-2 to 6
14	-20 to -14	-14 to -9	-9 to -6	-6 to -1	-1 to 7
15	-19 to -13	-13 to -8	-8 to -5	-5 to 0	0 to 8

Bones of *Eremotherium* are readily distinguished from the other sloths by their significantly larger size (Figure 5). The teeth have the distinctive square cross section and a parallel bilophodont occlusal surface of megatheres and an open pulp cavity with no distinct roots, characteristic of sloth teeth (Figure 6c).

Specimen IGM 14641 (U201) is a well-preserved palate with the alveoli of two molariform teeth, whose broken roots are included. The alveoli and remains of teeth have the rectangular to subquadrate occlusal outline of the bilophodont teeth of sloth. By their size, they we identified as belonging to *Eremotherium*. The other four cranial fragments are of the size and morphology expected for a large animal such as a giant sloth or proboscidean. Remains of both are found in this general area, so caution should be given to their identification. Given that they were all found in the same crack of the rock and at close proximity, we assume at least some could belong to the same individual.

The isolated molar and four appendicular elements were recovered from the Arrastre Lodoso section (Espinasa & Espinasa 2025). Periodic flooding within this passage reworks and redistributes fossil material. Hydraulic transport and depositional sorting result in bones being deposited loosely on the sediment surface or slightly embedded in clay banks (Figure 3). The molar has the rectangular to subquadrate occlusal outline of the bilophodont teeth of sloth, whose size identifies it as belonging to *Eremotherium*.

The shaft of the proximal end of the femur (Figure 8a) is anteroposteriorly flattened which distinguishes it from the similar sized late Pleistocene proboscideans in which the shaft of the femur is more circular. The indeterminate carpal IGM 14651 (U187) and podial IGM 14649 (U185) are referred to *Eremotherium* based on their large size and their morphology does not match the rectangular form seen in proboscideans.

Eremotherium is the largest known genus of extinct sloths, so it is readily distinguished from non-megathere sloths by size. *Eremotherium* has the greatest latitudinal range of all the extinct

Figure 5. Ungual phalanges (claws) from the third digit of the foot. a) *Eremotherium laurillardi*. IGM 14668 (R49). b) Megalonychid sloth cf. *Nohochichak* IGM 14674 (U100). c) *Eremotherium* ungual in the field to illustrate the size of specimen. All scales in cm.

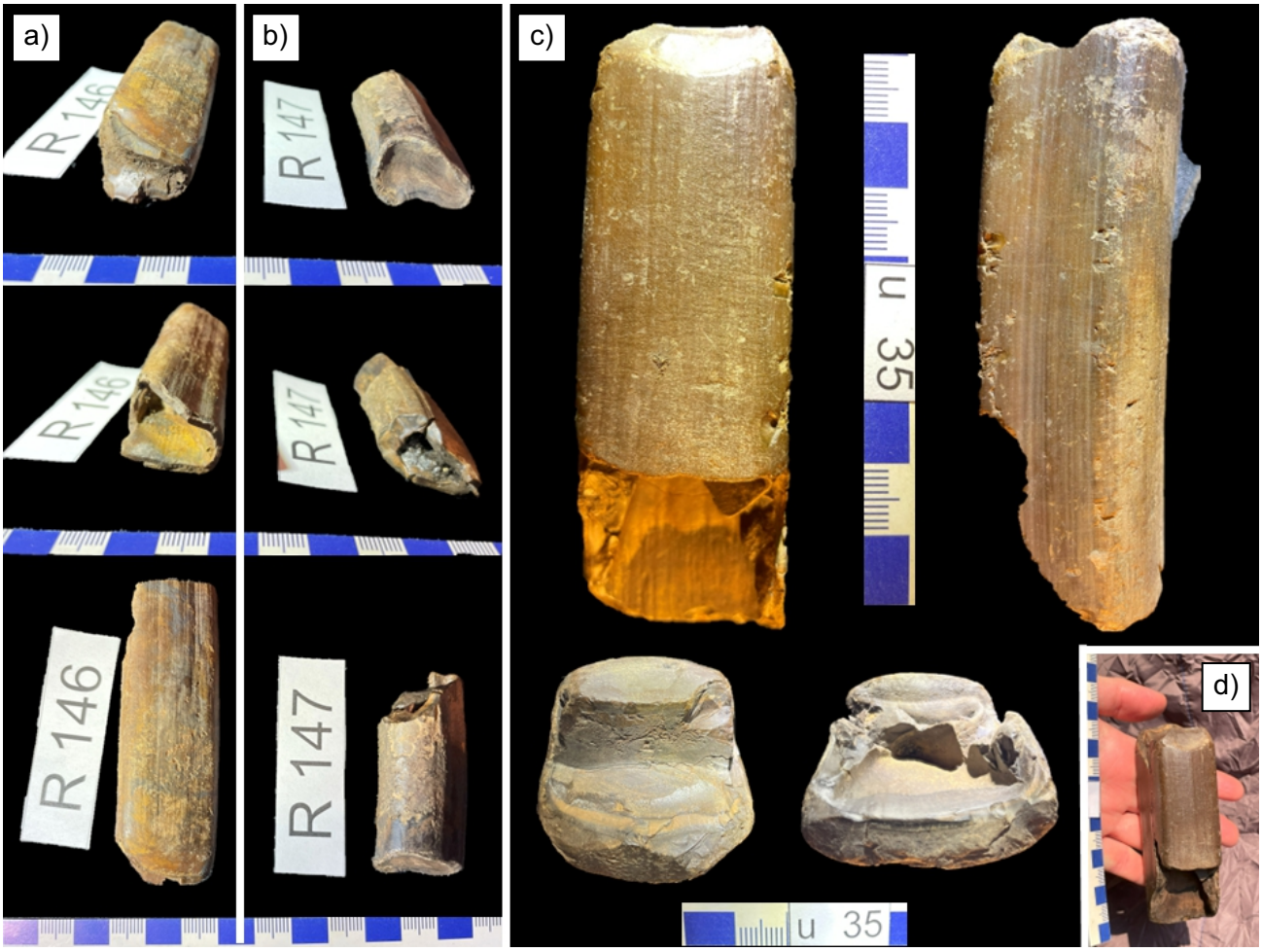

Figure 6. Teeth. a-b) Megalonychid cf. *Nohochichak* IGM 14670-14671 (R146-R147). c) *Eremotherium laurillardi* IGM 14669 (U35). d) *Eremotherium* tooth in hand to illustrate size of specimen. All scales in cm.

sloths with records from southern Brazil to New Jersey in the United States and has been referred to as the Pan-American sloth (Cartelle & De Iuliis, 1995). McDonald (2002) reported *Eremotherium* from 10 localities in Mexico but based on numerous subsequent discoveries (Carbot-Chanona *et al.*, 2022), the genus is now known from 34 localities including Sistema Calera cave. Based on its general distribution, *Eremotherium* appears to have lived primarily in tropical habitats. In Mexico, it is often found at higher elevations than in other parts of its range and the range of elevation of these localities is from 0-2500 meters above sea level. This wide elevational distribution of *E. laurillardi* in Mexico suggests that it may have inhabited a more diverse types of ecological regions, from coastal plains to open forests (Carbot-Chanona *et al.*, 2022).

While many sloths have been recorded from cave sites and it has been inferred that caves were used as denning sites (McDonald, 2003), the large size of *Eremotherium* precluded access to most caves and in the few caves from which it has been covered, such as Sistema Calera cave, its presence appears to be a taphonomic artifact of secondary transport of bones and teeth into the cave. Like many of the bones in Sistema Calera cave, the claws of *Eremotherium* (Figure 5a) show damage due to transport. The loss of teeth in the fragment of a right maxilla is also indicative of transport into the cave (Figure 7a). The isolated tooth has dimensions that match the alveoli in the maxilla fragment (Figure 7a–7c), but they were found over 150 m away from each other and in different galleries of the cave, so it is unlikely they are from the same individual.

Order Pilosa Flower, 1883
Suborder Folivora Delsuc *et al.*, 2001
Family Nothrotheriidae Ameghino, 1920
Genus *Nothrotheriops* Hoffstetter, 1954
Species *Nothrotheriops shastensis* Sinclair, 1905

Material: Vertebrae: 3380PF-64 (S05), 3380PF-65 (S56), 3380PF-28 (S85), and IGM 14652 (R42) Figure 9; Radius distal left: 3380PF-19 (S23) Figure 8f; Radius right: 3380PF-29 (S86) Figure 8d; Femur proximal right: IGM 14647 (R31) Figure 8b.

Remains were broadly scattered throughout the cave. They were found submerged under waters in the Llac Lluis lake or lying on top of the sediments of the Arrastre Lodoso gallery and the Upper-Level galleries (Espinasa & Espinasa 2025). Their distribution is due to the periodic flooding and redistribution of fossil material due to hydraulic transport.

Specimens are identified as belonging to *Nothrotheriops shastensis* because *Nothrotheriops* is the smallest of the late Pleistocene sloths in North America. While morphologically there is a general similarity in some parts of the post-cranial skeleton between nothrotheres and megalonychids, some the bones of Nothrotheriops such as the

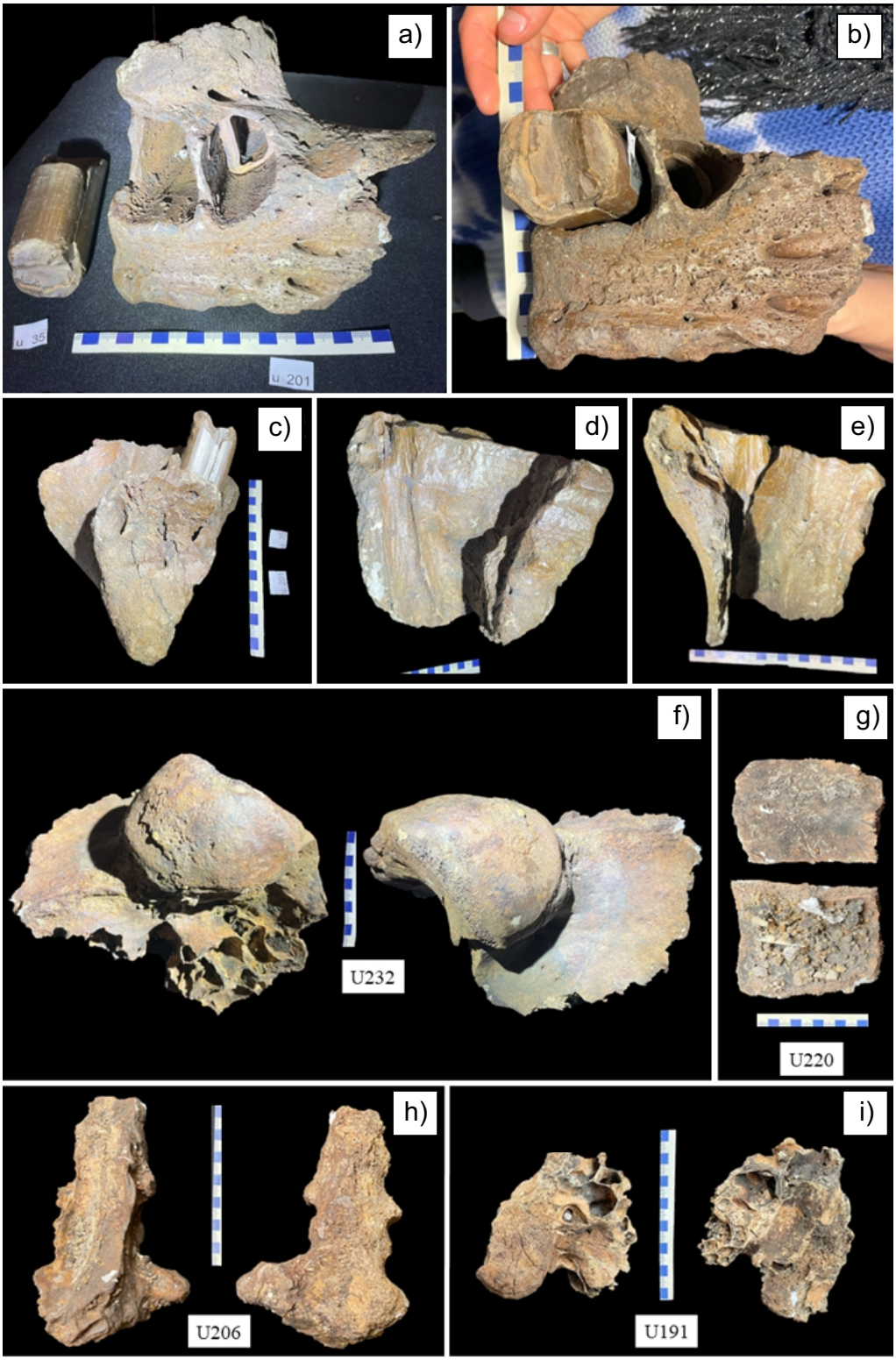

Figure 7. Fragments of skull of *Eremotherium laurillardi* IGM 14640-14644 (U191, U201, U206, U220 and U232). a) Fragment of skull (right maxilla with alveoli for first and second molariforms) by the side of tooth sample U35. Notice that in one of the alveoli there is a fragment of a tooth. b) Palate. Although the isolated molariform was collected in a separate part of the cave, its size fit well in the alveolus of the maxilla, suggesting they belong to an individual of similar size. c-e) Different views of the skull fragment. f-i) Skull fragments tentatively assigned to either *Eremotherium* or a Proboscidean. All scales in cm.

Figure 8. Long bones. a) Distal end of femur. *Eremotherium laurillardi.* 3380PF-60 (S35). b) Femur. Right proximal end of a sloth cf. *Nothrotheriups* IGM 14647 (R31). b) Tibia diaphysis of sloth, taxon indeterminate. IGM 14645 (R16). d) *Nothrotheriops* right radius. 3380PF-29 (S86). e) Megalonychid cf. *Nohochichak* diaphysis of left radius. IGM 14647 (R31). f) *Nothrotheriops* distal left radius. 3380PF-19 (S23). All scales in cm.

radius (Figures 8d and 8e) are more gracile compared those of the megalonychids.

Nothrotheriops is the smallest of the North American sloths. It first appears in North America in the Irvingtonian North American Land Mammal Age, represented by *N. texanus (*McDonald & Jefferson 2008). It was followed by the Rancholabrean species, *N. shastensis*. Given the Rancholabrean dates for Calera fossils, we assume the *Nothrotheriops* specimens at Sistema Calera cave belong to *N. shastensis*. McDonald (2002) listed 10 Rancholabrean localities for *Nothrotheriops* in Mexico and currently 13 localities are documented including Sistema Calera cave. *Nothrotheriops* is well represented in the Rancholabrean (McDonald & Jefferson, 2008) with a distribution from northern California through the southwestern United States and Mexico to Belize (De Iuliis *et al.*, 2015). While *Nothrotheriops* is most closely associated with desert habitat and its remains have been found in all four North American deserts, its preference of habitat appears to be somewhat flexible as it is known from caves in northern California and the asphalt deposits at Rancho La Brea. Many of the sites where *Nothrotheriops* has been found are cave sites, representing 33 (67 %) out of the 49 Rancholabrean records of the genus listed by McDonald and Jefferson (2008). In Mexico, six out of 13 (46 %), including Sistema Calera cave, are cave sites (McDonald & Jefferson, 2008 plus two unpublished reports) and the record from Belize is also a cave site (De Iuliis *et al.*, 2015). It appears that *Nothrotheriops* may have used caves as a maternal den based on the presence of bones of juveniles but also, given the low basal metabolism of sloths, caves may have also served as thermal refugia during seasonal extremes (McDonald, 2022). The topology of the entrances of Sistema Calera cave makes it unlikely that it was used as a den. Three out of four of the entrances are vertical and sometimes overhanging pits (Espinasa- Pereña *et al.*, 2024) that a sloth would have find difficult to descend or exit. The last entrance, Sótano del Toro, is a sinkhole that leads directly to a pool of water, with no dry horizontal galleries that could have been used as a den.

Order Pilosa Flower, 1883
Suborder Folivora Delsuc *et al.*, 2001
Family Megalonychidae Gervais, 1855
Genus cf. *Nohochichak* McDonald, *et al.*, 2017

Material. Anterior and lower left third molariforms: IGM 14670-14671 (R146-R147) Figures 6a-6b; Ungual phalange: IGM 14674 (U100) Figure 5b; Proximal femur: IGM 14647 (R31) Figure 8b.

All specimens were found in the Arrastre Lodoso Galery either lying on top of the sediments or embedded in clay by the wall (Figure 3). The megalonychid sloth is represented by two isolated teeth and one femur. They are smaller than the teeth of *Eremotherium*. The assignment to a megalonychid is based on the occlusal surface, which exhibits a triangular outline formed by the convergence of the mesial and distal lophs of the teeth. While *Megalonyx* is known from Mexico, the dimensions of the teeth are greater than those of the late Pleistocene species, *Megalonyx jeffersonii*.

The late Pleistocene record of megalonychid sloths in Mexico has recently expanded with several significant discoveries. These include *Meizonyx*, previously known only from El Salvador, now identified in the Sistema Huautla cave complex in the state of Oaxaca (McDonald *et al.*, 2020), as well as two newly described genera from submerged caves and cenotes on the Yucatán Peninsula: *Nohochichak* from Hoyo Negro in Quintana Roo (McDonald *et al.*, 2017), and *Xibalbaonyx* from a cenote near Puerto Morelos, Quintana Roo (Stinnesbeck *et al.*, 2017).

Pending the recovery of additional, more diagnostic material, we tentatively refer the megalonychid specimens from Sistema Calera cave to cf. *Nohochichak*, based on the similarity in teeth size and outline, which more closely resembles this genus than other known megalonychid taxa. If this provisional identification is confirmed, it would significantly extend the known geographic range of *Nohochichak*.

Order Cingulata Illiger, 1811
Family Chlamyphoridae Bonaparte, 1850
Subfamily Glyptodontinae Burmeister, 1879
Genus *Glyptotherium* Osborn, 1903
Species *Glyptotherium cylindricum* Brown, 1912

Material. Carapace osteoderms IGM 14656-14663 (R91-R98), IGM14655 (U216), IGM 14672 (R90), IGM 14672 (U215) Figure 10.

The isolated specimens were found in the pool by the entrance of Toro #2 and the plate with the attached 17 osteoderms was found at the Arrastre Lodoso gallery (Espinasa & Espinasa 2025).

The presence of *Glyptotherium* in Sistema Calera cave is based on osteoderms both isolated and associated (Figure 10). Zurita *et al.*, (2011) noted that the osteoderms in the genus are characterized by a primitive ornamentation pattern, consisting of a circular or subcircular central figure encircled by a row of polygonal peripheral figures. As in *Glyptodon*, the peripheral figures are always smaller than the central one. What distinguishes the osteoderms in *Glyptotherium* is the extremely rugose texture of the external surface while in *Glyptodon* it is almost smooth (Ameghino, 1889; Soibelzon *et al.*, 2006). Additionally, in *Glyptotherium* there are numerous perforations, and the peripheral figures may be less symmetrical in some osteoderms with some portions of the carapace having perforations that are more evident and form a distinct oblique dorsoventral orientation.

Although closely related to the South American genus *Glyptodon*, North American glyptodonts are distinct from their South American relatives and placed in their own genus *Glyptotherium* (Gillette & Ray, 1981; Zurita *et al.*, 2018). Multiple species of the North America genus have been described from their first appearance in the late Pliocene (Blancan NALMA) until their extinction at the end of the Rancholabrean NALMA. Three species of *Glyptotherium* have previously been recognized from Mexico: *G. floridanum*, *G. cylindricum* and *G. mexicanum*. The type of *G. mexicanum* was reported as missing by Gillette and Ray (1981), who noted that portions of the description of the type included pampathere material, which raised questions as to its validity. Subsequently, Carranza-Castañeda and Miller (1987) reported the rediscovery of part of the type, the carapace (IGM 4006), although the skull, sacrum and isolated teeth are still missing. Most of the lower jaw with incomplete dentition was recovered with the carapace but whether it is part of the original type described by Cuatáparo and Ramirez (1875) could not be determined. While numerous new records of *Glyptotherium* from Mexico have been published since 1987, none appear to have taken the holotype of *G. mexicanum* into account other than Brown (1912), who placed it in a distinct genus, *Brachyostracon*, but this genus is now considered a junior synonym of *Glyptotherium* (Osborn, 1903).

While a detailed examination of the taxonomic relationship between *Glyptotherium cylindricum* and *G. mexicanum* is beyond the scope of this paper, in this study we follow the recent synonymy of *G. floridanum* with *G. cylindricum* (Ramírez-Cruz & Montellano-Ballesteros 2014), along with the recognition that future research incorporating the previously overlooked type specimen of *G. mexicanum* may ultimately result in *G. cylindricum* being recognized as its junior synonym.

Glyptotherium cylindricum is sufficiently distinctive from other species of the genus that it is considered a valid species by Cuadrelli *et al.*, (2018). Based on new finds from Tamaulipas and Tlaxcala, Ramírez-Cruz and Montellano-Ballesteros (2014) determined

Figure 9. *Nothrotheriops* vertebrae 3380PF-64 (S05), 3380PF-65 (S56), 3380PF-28 (S85), and IGM 14652 (R42) in oblique and posterior view. S56, S85 and R042 are posterior thoracic vertebrae. Sscale in cm.

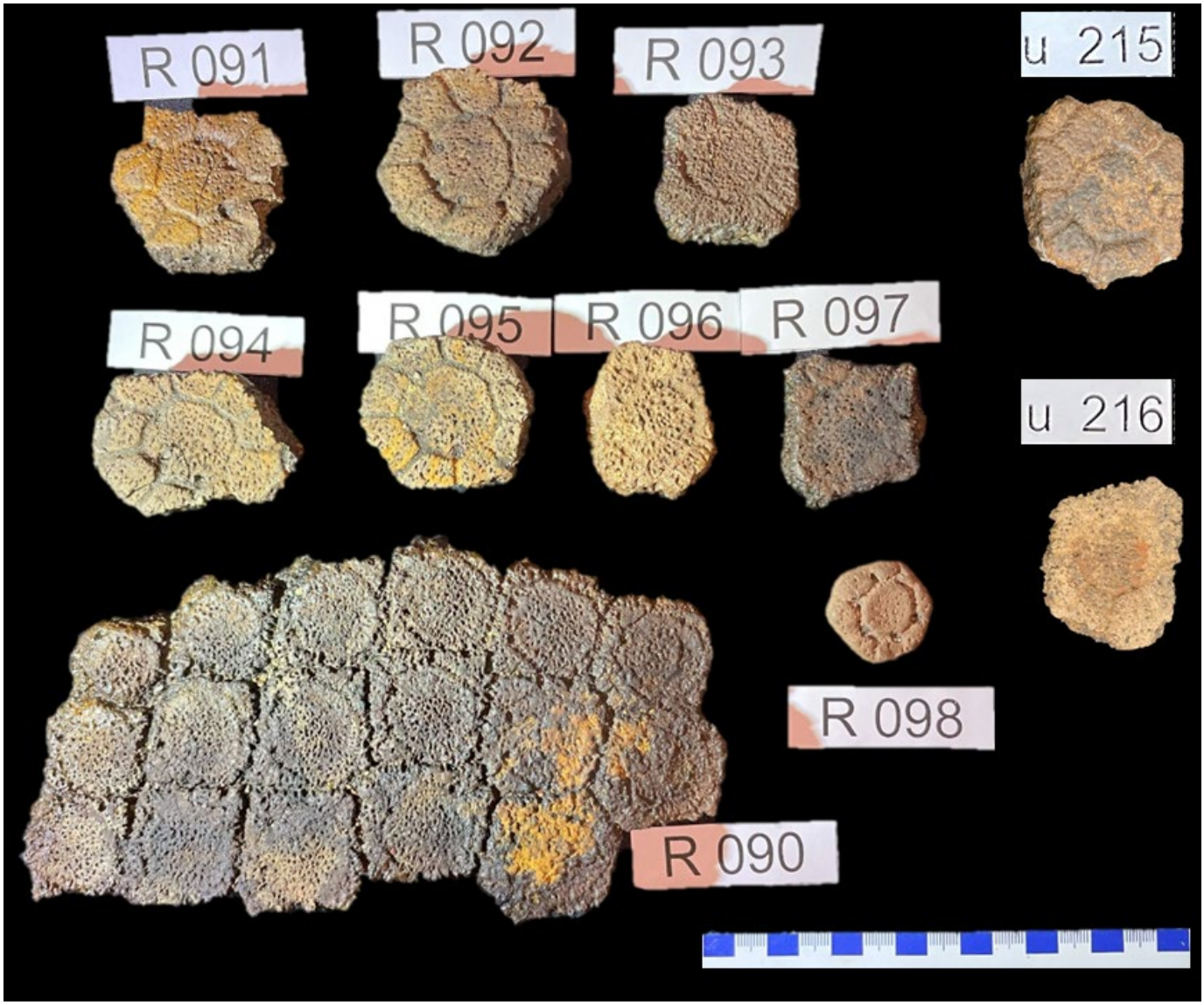

Figure 10. Osteoderms of glyptodont (*Glyptotherium cylindricum*). IGM 14656-14663 (R91-R98), IGM14655 (U216), IGM 14672 (R90), IGM 14672 (U215). Scale in cm.

there are not enough characters to differentiate *G. floridanum* from *G. cylindricum* and considered the two taxa synonymous, with *G. cylindricum*, having nomenclatural priority. This conclusion is in keeping with the observations of Gillette (pers. com.) that *Glyptotherium* had little or no evolution after the origin of the genus, a condition he recognized as evolutionary stasis. Accepting the synonymy of *G. floridanum* (Simpson, 1929) with *G. cylindricum* (Brown, 1912), all previous records of *G. floridanum* in Mexico and the United States greatly enlarges the number of records of this species and consequently the distribution of *G. cyclindricum*, including records in Central America such as Guatemala described by Cuadrelli *et al.*, (2018). This essentially reduces the diversity of glyptodonts in the late Pleistocene of North America to a single species.

Following the previously discussed taxonomic changes proposed by Cuadrelli *et al.*, *(*2018) the distribution of *G. cylindricum* is now more widespread than previously thought. The northernmost records in North America are in Texas and Florida. The type locality is near Ameca, Jalisco, Mexico (Brown, 1912) and other localities in Mexico include the states of Aguascalientes, Chiapas, Hidalgo, Jalisco, the State of Mexico, Nuevo León, Oaxaca, Puebla, Veracruz, Sonora, San Luis Potosí, Tamaulipas and Tlaxcala (Bravo-Cuevas *et al.*, 2009, Ferrusquıa-Villafranca *et al.*, 2010, Ramırez-Cruz & Montellano-Ballesteros, 2014, Sánchez Salinas *et al.*, 2016). The Sistema Calera cave record falls well within the known distribution of the species in Mexico. All Late Pleistocene glyptodonts from Central America are assigned to *Glyptotherium* sp. They include specimens from El Salvador (Webb & Perrigo, 1984), *G. floridanum* from Costa Rica (Valerio *et al.*, 2005), Honduras (Lucas, 2008), Panama (Lucas, 2014) or *Glyptotherium arizonae*, also from El Salvador (Cisneros, 2005). These identifications are based on limited records, primarily isolated osteoderms and molariform teeth. Based on the recovery of a fairly complete skeleton with good stratigraphic context from Guatemala, Cuadrelli *et al.* (2023) proposed that these previous taxonomic assignments should be changed to *G. cylindricum* and that this species is limited chronologically to the Rancholabrean. *Glyptotherium cylindricum* is also considered to be present in South America (Cuadrelli *et al.*, 2023), with records in Venezuela (Falcón State) and Brazil (States of Pernambuco, Grande do Norte and Minas Gerais).

Carbon isotope values and estimated resource use

The carbon isotopic signature ($\delta^{13}C$) from bones of the studied mammals varied between -11.4 ‰ (considering the trophic corrections of -1.5 ‰ in omnivore and carnivores) to -4.2 ‰. This data supports that the fauna lived between 8000 to 31000 cal yr BP in three main types of vegetation they fed on; low-density forests, an arboreal savanna, and in an ecotone between arboreal savanna to open savanna (Figure 11).

All taxa *Eremotherium laurillardi*, *Tremarctos* cf. *floridanus*, *Mammuthus columbi*, *Glyptotherium cyclindricum*, and *Bison* sp. were mixed-feeders "browsers", feeding more on C_3 plants (p_i = 51–100 %; Table 1). Both the dire wolf, *Canis dirus*, and the saber-toothed cat, *Smilodon fatalis*, show similar carbon isotopic signatures, with $\delta^{13}C$ values of -5.5 ‰ (Table 1). These values suggest that both predators consumed prey that occupied broadly similar habitats. However, they were not contemporaneous in the study area, as they occurred at different times, approximately 13 ka and 31 ka, respectively (Table 1). At Sistema Calera cave, *Canis dirus* lived during the same period (12–13 ky; Table 1) as *Mammuthus columbi*, *Glyptotherium cyclindricum* and *Tremarctos* cf. *floridanus*. Between these, only *M. columbi* (p_i = 40 %; Table 2) and *G. cylindricum* (p_i = 60 %; Table 2) could be potential contributors for the carbon isotopic signature of *Canis dirus*. Considering a mean body mass of 60 kg for the dire wolf (Anyonge & Roman, 2006) it could prey on animals between 80 to 877 kg, thus, *G. cyclindricum* (mean body mass = 375 kg; Carlini *et al.*, 2022) was in the range to be actively hunted for *C. dirus*, while, for *M. columbi*, due its large size (maximum body mass = 10 ton; Jiménez-Moreno *et al.*, 2022) could only have potentially preyed on immature mammoths or was able to include mammoth in its diet by scavenging.

DISCUSSION AND CONCLUSIONS

The diversity of xenarthrans from Sistema Calera cave is unique in that it is only the second site in which *Nothrotheriops* is found in the same locality as *Eremotherium* and *Glyptotherium*. Admittedly, *Eremotherium* and *Glyptotherium* from Calera have been dated to different ages (23000–24000 yr bp *vs.* 12000–13000 yr bp) and the *Nothrotheriops* has not yet been dated, so it is uncertain if they cohabitated with each other in the region. Although the range of *Nothrotheriops* extended into Mexico and further south into Belize (De Iuliis *et al.*, 2015), as well as recent reports of the presence of the genus in South America, Argentina (Brandoni & Vezzosi, 2019) and Uruguay (Varela *et al.*, 2023), there are no previous reports of the co-occurrence for the three taxa within Mexican faunal assemblages, despite the potential for such associations.

During the late Rancholabrean in the United States, the geographic range of *Nothrotheriops* was primarily confined to the Southwest and the West Coast. In the United States the range of *Eremotherium* extended primarily along the Gulf Coast to Florida and northward along the Atlantic Coast. The difference in their ranges reflects significant differences in their paleoecology and diet. *Nothrotheriops* is associated with primarily a dry arid environment and based on coprolites had a diet predominately of desert vegetation (Hansen, 1978). In contrast, based on stable isotopes, the preferred habitat of *Eremotherium* is tropical to subtropical and a generalist mixed feeder (Omena *et al.*, 2021). The only previous record of these two taxa found associated in a fauna is the Wright gravel pit on the Nueces River, Nueces County, Texas (Sagebiel, 2022). The fauna from the Wright gravel pit also includes the cingulates, *Glyptotherium floridanum* and *Holmesina sepentrionalis*. This unique assemblage reflects its location which is at the extreme eastern margin of the Rancholabrean distribution of *Nothrotheriops* within the USA and the extreme western margin of the Rancholabrean distribution of *Eremotherium*, *Glyptotherium* and *Holmesina*. The association of *Nothrotheriops* and *Glyptotherium* parallels that of *Nothrotheriops* and *Eremotherium*. The northern part of the distribution of *Glyptotherium* is also along the Gulf Coast of Texas to Florida and onto the Atlantic Coast although it does not extend as far north as *Eremotherium* on the Atlantic Coast.

Data supports habitat partitioning, with *Nothrotheriops* and *Eremotherium* identified as mixed-feeding browsers and *Glyptotherium* as a mixed-feeding grazer. The stable isotope values in *Nothrotheriops* (p_iC_3 = 82%, p_iC_4 = 18%; Dantas *et al.*, 2023 and references therein) and *Eremotherium* (p_iC_3 = 62%, p_iC_4 = 38 %; Pérez-Crespo *et al.*, 2015) indicate both taxa were mixed-feeder "browsers". Vegetation preserved in the dung of *Nothrotheriops* corroborates that in this species, its diet was of a mixed-feeder "browser" dominated by desert adapted plants (Hansen, 1978). *Glyptotherium* is considered a mixed-feeder "browser" with a diet dominated by C_3 plants (p_iC_4 = 55 %). The available isotopic data from the Cedral glyptodont, in Mexico,

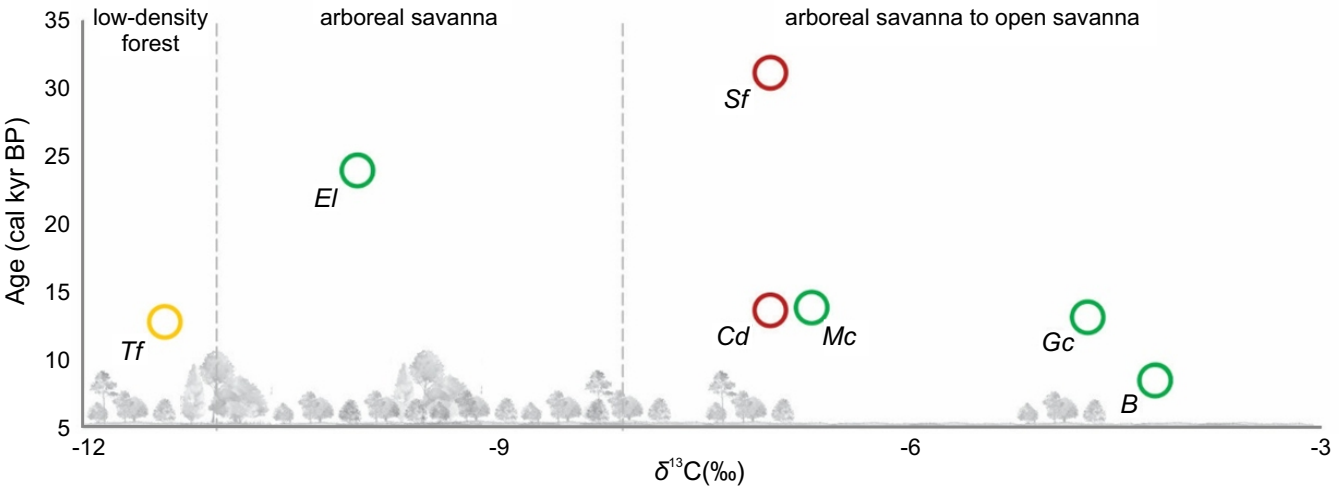

Figure 11. Bi-plot graphic of $\delta^{13}C$ V-PDB signatures from bone samples and calibrated age (cal yr BP) for the Late Pleistocene mammals from Sistema Calera cave and the habitats in which they lived. Labels: Herbivores (green circles): *El - Eremotherium laurillardi*, *Mc - Mammuthus columbi, Gc - Glyptotherium cyclindricum, B – Bison* sp.; Omnivore (orange circle): *Tf - Tremarctos* cf. *floridanus;* Carnivores (red circles): *Sf – Smilodon fatalis*, *Cd – Canis dirus*.

indicates it ate mainly grasses ($\delta^{13}C = -4.3 \pm 0.5$ ‰) and lived in open areas close to water sources (Pérez-Crespo *et al.*, 2012). The $\delta^{13}C$ value of the Sistema Calera cave *Eremotherium* ($\delta^{13}C = -10.0$ ‰, Table 1) and *Glyptotherium* ($\delta^{13}C = -4.7$ ‰, Table 1) are similar to those available for other localities in Mexico (Pérez-Crespo *et al.*, 2012; Pérez-Crespo *et al.*, 2015) indicating a consistency in habitat preference.

As the fossil assemblage in Sistema Calera cave is time averaged, it is possible that the association of *Nothrotheriops* with *Eremotherium* and *Glyptptherium* is spurious, and they were in the vicinity of the cave at different times when there was a difference in the vegetation. The range of dated specimens at Sistema Calera cave spans a minimum of 22000 years, from a maximum of 31027–31178 cal yr BP of *Smilodon* (IGM 14679; U36) to 8423–8549 cal yr BP for *Bison* (IGM 14675; S108), which post-dates the extinction of the North American megafauna represented by the sloths and the glyptodont.

The *Glyptotherium* specimen (IGM 14673; U215) from Sistema Calera cave is the only glyptodont with a direct radiocarbon age permitting a calibrated radiocarbon age of 12759–12998 cal yr BP, placing it near the onset of the Younger Dryas. In contrast, the *Eremotherium* specimen (IGM 14641; U201) dates to 23305–23761 cal yr BP, corresponding to the Last Glacial Maximum. Given the likely changes in vegetation between these two climatic periods, the presence of both species at the site can reasonably be attributed to their occupation of the cave vicinity during distinct intervals, each characterized by different plant communities. However, to definitively rule out the possibility that *Glyptotherium* and *Eremotherium* were contemporaneous in the region, additional radiocarbon dates are necessary. Due to the absence of clear stratigraphy in the cave and the potential for specimen mixing from episodic flooding, it remains impossible to reconstruct a reliable faunal succession or document environmental changes in the cave's surroundings without a more extensive and well-dated assemblage.

Another possible explanation for the high vertebrate diversity at Sistema Calera cave is the geographic setting of the Sierra de El Abra, a limestone range located on the eastern flank of the Sierra Madre Oriental in northeastern Mexico. This range serves as a biogeographic contact zone, where Nearctic and Neotropical floras and faunas converge, fostering exceptional species richness. To the west lies the Altiplano Mexicano, a high-elevation plateau, while to the east is the Gulf Coastal Plain. This transitional position, combined with its complex karst topography, contributes to the ecological heterogeneity that nowadays supports such a diverse faunal and floral assemblage (Sahagún-Sánchez & De-Nova, 2020).

Today, the Sierra de El Abra is predominantly covered by tropical dry forest, yet its complex combination of elevation gradients, slope orientation, and karstic topography creates a diverse mosaic of microhabitats that support both tropical and temperate species. On the eastern slopes and within sheltered canyons, the Neotropical vegetation includes palms, cycads, and evergreen hardwoods. The western slopes and higher elevations are dominated by Nearctic flora such as oaks, pines, agaves, and thorn scrub. Vegetation at the base of the Sierra is mainly thornscrub (mezquital), where woody plants like mesquite, acacia, and cacti dominate, but grasses are common in open areas. A similar ecological mosaic likely existed during the Pleistocene, creating a dynamic landscape where a variety of browsers and grazers could coexist near the entrance of the cave, each adapted to the interdigitated niches provided by the overlapping vegetation zones.

Lastly, with regards to the megalonychid sloth cf. *Nohochichak*, the limited material precludes any real conclusions about its ecology. This taxon was originally recovered from Hoyo Negro in the Actun Sac cave system in Quintana Roo on the Yucatan Peninsula and this is only the potentially second record of the genus. Its presence in Sistema Calera cave in San Luis Potosí greatly enlarges the potential range of this sloth and with additional specimens it potentially should provide a basis for a better understanding of its paleoecology and faunal associates.

Paleoecology of *Glyptotherium*

The presence of *Glyptotherium* at Sistema Calera cave deserves further analysis. Although the current dataset is limited and additional sites are needed, there appears to be a general trend in which *Glyptotherium* occurs at progressively higher elevations from the southern United States through Mexico to Panama, corresponding with the lower southern latitude (Figure 12). *Glyptotherium cylindricum* in Guatemala has been found at elevations up to 2400 m above sea level and are among the highest elevations reported for the genus (Cuadrelli *et al.*, 2023). Many other records of the glyptodont in Mexico are at high elevations comparable to Guatemala, including Pachuca-Tulancingo, State of Hildago, which is at 2458 m a.s.l. (Bravo-Cuevas *et al.*, 2009) and Tequixquiac in the State of Mexico, at 2350 m a.s.l. (Cuatáparo & Ramirez, 1875). Since mean annual temperatures tend to be cooler at higher latitudes and elevation, with warmer temperatures closer to the equator, this would allow the glyptodont to move to higher elevations, although possibly only seasonally (Figure 12).

Sistema Calera cave, at an elevation of 103 m a.s.l., is considerably lower than most sites at this latitude and illustrates the range of elevation inhabited by *Glyptotherium* at different latitudes (Figure 12). For example, the Cedral palaeontological site, which is also located in the state of San Luis Potosí, México, is at 1700 m a.s.l. (Pérez-Crespo *et al.*, 2012). The *Glyptotherium* from El Cedral was found under sediments dated to ^{14}C 31850 ± 1600 (Pérez-Crespo *et al.*, 2012). Given the apparent incongruency that the El Cedral specimens lived at an older and colder stage of the ice age, and at a higher altitude than the Sistema Calera cave, other ecological alternatives should be examined. As mentioned before, the $\delta^{13}C$ V-PDB values for the El Cedral specimen had a mean of -4.32 ‰ and a standard deviation of 0.51 ‰ (Pérez-Crespo *et al.*, 2012). The Sistema Calera cave was -4.7, suggesting that in both sites, despite the difference in age and altitude, *Glyptotherium* had access to similar resources needed for a mixed-feeder "grazer".

Besides the possible southward shift in the glyptodonts range concurrent with climatic cooling during the late Pleistocene, there could also be an elevational shift in its distribution from higher elevations during interglacials or interstadials to lower elevations during colder intervals. The presence of the glyptodont at Sistema Calera cave may be thus linked to being dated to just prior the Younger Dryas Period. Confirmation of this possibility will require a higher resolution chronology to see if there is a correlation between increase or decrease in mean average temperatures and the highest and lowest elevations at which the glyptodont occurs.

As noted, the range of *Glyptotherium* includes topographically diverse habitats, more so in Mexico and Central America, than in the United States where the late Pleistocene records are primarily known from lower elevations along the Gulf Coastal Plain of Texas and Florida, neither of which have significant changes in topography with an average elevation of 518 meters in Texas and a maximum elevation of 105 meters in Florida. In areas with significant differences in topography, large herbivores often make vertical seasonal migrations. In temperate regions, the vertical movement of cervids from a low-elevation winter range to a high-elevation summer range is the most common pattern of migration as forage quality increases at high elevations. The summer migration to higher elevations is considered a strategy that increases the energy intake among northern temperate ungulates (Mysterud *et al.*, 2001). It is possible however that glyptodonts as well as sloths in these areas also undertook such

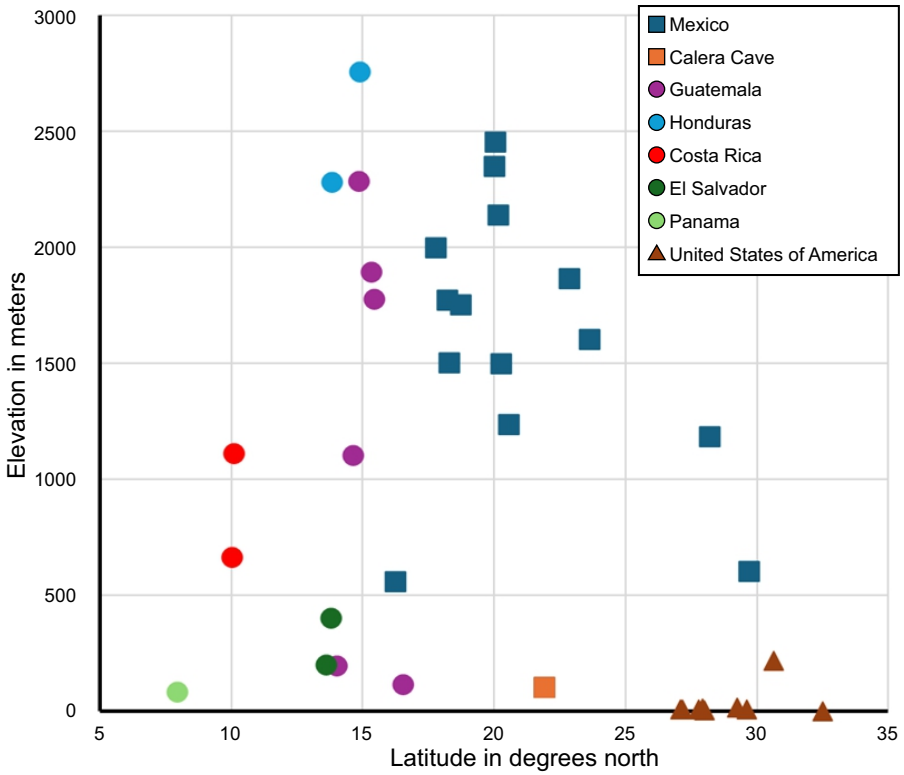

Figure 12. Plot of latitude and elevation of *Glyptotherium* fossil localities, showing a trend of the glyptodont being able to inhabit higher elevations at more southern latitudes. The Sistema Calera cave is at low altitude.

seasonal migrations up and down the Sierra Madre Oriental to obtain higher quality forage that was easier to digest.

Climate likely played a key role in range shifts and extinction, including glyptodonts. Ecological models (Magoulick *et al.*, 2025) indicate suitable habitats across Central America and suggest possible north–south shifts in its range during the Rancholabrean. The model also supported previous hypotheses by Gillette and Ray (1981) that the ecology and distribution of *Glyptotherium* was constrained by the need for a warm, wet environment. The stable isotope data supports the interpretation that savanna was the preferred habitat of *Glyptotherium*. Further study is needed to clarify the role of the Central American Filter and how savanna expansion and contraction influenced the taxa involved in the Great American Biotic Interchange (GABI) (Webb, 1978).

Cuadrelli *et al.*, (2023) proposed a progressive retraction of the geographical range of the glyptodont during the Late Pleistocene, with its distribution shifting over time in response to climatic and environmental changes associated with the last glacial period. Oliveira *et al.*, (2010) proposed that the presence of *Glyptotherium* in northeastern Brazil during the Late Pleistocene OIS 3 (60–26 ka) was potentially related to the middle Wisconsin interstadial event.

Acknowledgments. Marist University, Scurion, Pigeon Mountain Industries (PMI), and Stenlight for partially supporting field work. MATD thanks to Conselho Nacional de Desenvolvimento Científico e Tecnológico CNPq for financial support for Project INCT Paleovert (process 406902/2022-4) and research fellowship (process 304394/2023-8).

Author contributions. H. Gregory McDonald: Identification and description of sloth material, reviewed manuscript. Mário A.T. Dantas: Description of dated material, reviewed manuscript. Ramón Espinasa-Pereña: Safeguarding of material, reviewed manuscript. Luis Espinasa: PI, field work, wrote manuscript, Identification of material.

Declaration of competing interests. All authors have no possible interests that could be perceived as influencing the submitted work.

Data availability statement. Original fossil material can be viewed at the collections of the Instituto de Geología (IGM), Universidad Nacional Autónoma de México (UNAM), and the Sociedad Mexicana de Espeleología Mexicana upon request. Original photos other than the ones included in the article can be viewed in https://drive.google.com/drive/folders/1AU7lvOrz_T4dlsfZmgTtFiE4cSKgcJ64?usp=sharing Further access to other original data can be shared upon request to corresponding author.

REFERENCES

Ameghino, F. (1889). Contribución al conocimiento de los mamíferos fósiles de la República Argentina. *Actas de la Academia Nacional de Ciencias de Córdoba*, 6, 1e1027. doi.org/10.5962/bhl.title.121288

Ameghino, F. 1920. Sur les édentés fossiles de l' Argentine. Examen critique, révision et correction de l' ouvrage de M. R. Lydekker "The exinct edentates of Argentina", etc. (Ouvrage à démiinédite avec des notes additionelles sur quelques ongulés et carnassiers). In: A.J. Torcelli (Ed.) Obras Completas y Correspondencia Científica de Florentino Ameghino, Taller de Impresiones Oficiales del Gobierno de la Provincia de Buenos Aires, 11: 447– 909.

Anyonge, W., & Roman, C. (2006). New body mass estimates for Canis dirus, the extinct Pleistocene dire wolf. *Journal of Vertebrate Paleontology*, *26*(1), 209–212. doi.org/10.1671/0272-4634(2006)26[209:nbmefc]2.0.co;2

Bell, C. J., Lundelius Jr., E. L., Barnosky, A. D., Graham, R. W., Lindsey, E. H., Ruez, Jr., D. R., Semken Jr., H. A., Webb, S. D., & Zakrzewski, R. J. (2004). *The Blancan, Irvingtonian and Rancholabrean Mammal Ages. Late*

Cretaceous and Cenozoic Mammals of North America: Biostratigraphy and Geochronology. Columbia University Press, New York, 232-314.

Bocherens, H., Koch, P. L., Mariotti, A., Geraards, D., & Jaeger, J. J. (1996). Isotopic biogeochemistry (^{13}C, ^{18}O) of mammalian enamel from African Pleistocene hominid sites. *Palaios*, *11*, 306–318. doi.org/10.2307/3515241

Bonaparte, C. L. (1850). Conspectus systematis Mastozoologiae. *Nuovi Annali delle Scienze Naturali*, *3*, 472-475.

Bonet, F. (1952). La facies urgoniana del Cretácico Medio de la región de Tampico. *Boletín Asociación Mexicana Geólogos Petroleros*, *4*(5-6), 153–262.

Bonet, F. (1963). Biostratigraphic notes on the Cretaceous of eastern Mexico. *Corpus Christi Geological Society Annual Field Trip Guidebook*, *Peregrina Canyon and Sierra de El Abra*, *Mexico*, 36–48.

Bonilla Díaz, C. (2018). *Paleoecología del Pleistoceno tardío en la Cueva La Presita (San Luis Potosí*, *México)* [Tesis de Licenciatura]. Mexico, Benemérita Universidad Autónoma de Puebla.

Brandoni, D. & Vezzosi, R. I. (2019). *Nothrotheriops* sp. (Mammalia, Xenarthra) from the Late Pleistocene of Argentina: implications for the dispersion of ground sloths during the Great American Biotic Interchange. *Boreas*, *48*, 879–890. doi.org/10.1111/bor.12401

Bravo-Cuevas, V. M., Ortiz-Caballero, E. & Cabral-Perdomo, M. A. (2009). Gliptodontes (Xenarthra, Glyptodontidae) del Pleistoceno Tardıo (Rancholabreano) de Hidalgo. Centro de Mexico. *Boletin de la Sociedad Geológica Mexicana*, 61, 267–276. doi.org/10.18268/bsgm2009v61n2a14

Bregman, R. (1988). Forms of seed dispersal in Cactaceae. *Acta Botanica Neerlandica*, *37*(3), 395–402. doi.org/10.1111/j.1438-8677.1988.tb02148.x

Brown, B. (1912). *Brachyostracon*, a new genus of glyptodont from Mexico. *Bulletin of the American Museum of Natural History*, *31*, 167–177.

Burmeister, H. (1879). Description physique de la République Argentine. Tome III. Mammifères fossiles. Buenos Aires.

Carbot-Chanona, G., Gómez-Pérez, L. E. & Coutiño-José, M. A. (2022). A new specimen of *Eremotherium laurillardi* (Xenarthra, Megatheriidae) from the Late Pleistocene of Chiapas, and comments about the distribution of the species in Mexico. *Boletín de la Sociedad Geológica Mexicana*, *74*(2), 1–12. doi.org/10.18268/bsgm2022v74n2a070322

Carlini, A. A., Carrillo-Briceño, J. D., Jaimes, A., Aguilera, O., Zurita, A. E., Iriarte, J., & Sánchez-Villagra, M. R. (2022). Damaged glyptodontid skulls from Late Pleistocene sites of northwestern Venezuela: evidence of hunting by humans?. *Swiss Journal of Palaeontology*, *141*(1), 11. doi.org/10.1186/s13358-022-00253-3

Carranza-Castañeda, O. & Miller, W. E. (1987). Rediscovered type specimens and other important published Pleistocene mammalian fossils from Central Mexico. *Journal of Vertebrate Paleontology*, *7*(3), 335–341. doi.org/10.1080/02724634.1987.10011664

Carrillo-Bravo, J. (1971). La plataforma Valles-San Luis Potosí: *Boletín Asociación Mexicana de Geólogos Petroleros*, *23*(1-6), 1–113.

Cartelle, C. & De Iuliis, G. (1995). *Eremotherium laurillardi*: the Panamerican late Pleistocene megatheriid sloth. *Journal of Vertebrate Paleontology*, *15*(4), 830–841. doi.org/10.1080/02724634.1995.10011265

Cerling, T. E. & Harris, J. M. (1999). Carbon isotope fractionation between diet and bioapatite in ungulate mammals and implications for ecological and paleoecological studies. *Oecologia*, *120*, 347–363. doi.org/10.1007/s004420050868

Cerling, T. E., Harris, J. M., Hart, J. A., Kaleme, P., Klingel, H., Leakey, M. G., Levin, N. E., Lewison, R. L., & Passey, B. H. (2008). Stable isotope ecology of the common hippopotamus. *Journal of Zoology*, *276*(2), 204–212. doi.org/10.1111/j.1469-7998.2008.00450.x

Cherkinsky, A. (2009). Can We Get a Good Radiocarbon Age from "Bad Bone"? Determining the Reliability of Radiocarbon Age from Bioapatite. *Radiocarbon*, 51(2), 647–655. doi.org/10.2458/azu_js_rc.51.3523

Christiansen, P., & Harris, J. M. (2005). Body size of *Smilodon* (Mammalia: Felidae). *Journal of Morphology*, *266*(3), 369–384. doi.org/10.1002/jmor.10384

Cisneros, J. C. (2005). New Pleistocene vertebrate fauna from El Salvador. *Revista Brasileira de Paleontologia*, (8), 239–255. doi.org/10.4072/rbp.2005.3.09

Coplen, T. B. (1994). Reporting of stable hydrogen, carbon, and oxygen isotopic abundances. *Pure and Applied Chemistry*, *66*(2), 273–276. https://doi.org/10.1351/pac199466020273

Cuadrelli, F., Zurita, A. E., Toriño, P., Miño-Boilini, Á. R., Rodríguez-Bualó, S., Perea, D. & Acuña Suárez, G.E. (2018). Late Pleistocene Glyptodontinae (Mammalia, Xenarthra, Glyptodontidae) from southern South America: a comprehensive review. *Journal of Vertebrate Paleontology*, *38*(5), p.e1525390. doi.org/10.1080/02724634.2018.1525390

Cuadrelli, F., Escamilla, J., Zurita, A., Gillette, D. D. & Dávila, L.S. (2023). *Glyptotherium cylindricum* (Cingulata, Glyptodontidae) from the Late Pleistocene of Guatemala: the most complete record of Glyptodontinae from Central America. *Alcheringa: An Australasian Journal of Palaeontology*, *47*(3), 336–347. doi.org/10.1080/03115518.2023.2242440

Cuatáparo, J. N. & Ramirez S. (1875). Descripción de un mamífero fósil de especie desconocida, perteneciente al género *Glyptodon*, encontrado en las capas posterciarias de Tequixquiac, en el Distrito de Zumpango. *Sociedad Mexicana de Geografía y Estadística Boletín*, *2*, 354–362.

Dantas, M. A. T., & Cherkinsky, A. (2023). Interrelation of radiocarbon ages from bone fractions in the Brazilian Intertropical Region. *Quaternary Research*, *115*, 202–206. doi.org/10.1017/qua.2023.19

Dantas, M. A. T., Campbell, S. C., & McDonald, H. G. (2023). Paleoecological inferences about the Late Quaternary giant sloths. *Journal of Mammalian Evolution*, *30*(4), 891–905. doi.org/10.1007/s10914-023-09681-5

De Iuliis, G., McDonald, H.G., Stanchly, N., Spenard, J., & Powis. T. G. (2015). *Nothrotheriops shastensis* (Sinclair, 1905) from Actun Lake: First record of Nothrotheridae (Mammalia, Xenarthra, Pilosa) from Belize. *Ameghiniana*, 52(1), 153-171. doi.org/10.5710/amgh.05.11.2014.2821

Delsuc, F., Catzeflis, F. M., Stanhope, M. J., & Douzery, E. J. P. (2001). The evolution of armadillos, anteaters and sloths depicted by nuclear and mitochondrial phylogenies: implications for the status of the enigmatic fossil *Eurotamandua. Proceedings of the Royal Society B: Biological Sciences*, 268, 1605–1615.

Domingo, L., Prado, J. L., & Alberdi, M. T. (2012). The effect of paleoecology and paleobiogeography on stable isotopes of Quaternary mammals from South America. *Quaternary Science Reviews*, *55*, 103–113. doi.org/10.1016/j.quascirev.2012.08.017

Elliot, W. R. (2018). The *Astyanax* Caves of Mexico, Cavefishes of Tamaulipas, San Luis Potosí, and Guerrero. *Association for Mexican Cave Studies Bulletin*, 26.

Espinasa, L., & Espinasa, M. (2015). Hydrogeology of caves in the Sierra de El Abra Region. Chapter 2, In: A. C., Keene, M., Yoshizawa, & S. E., McGaugh (eds.), *Biology and Evolution of the Mexican Cavefish* (pp. 41–58). Amsterdam, Academic Press (Elsevier). doi.org/10.1016/B978-0-12-802148-4.00002-5

Espinasa, L., & Espinasa, J. (2025). Crypt of the Megafauna. *Association for Mexican Cave Studies. Bulletin*, 27.

Espinasa-Pereña, R., Espinasa-Diamant, S., Diamant, R., McDonald, H. G., Soriano, J. A., & Espinasa, L. (2024). Discovery of a Pleistocene megafaunal assemblage in a cave in Sierra de El Abra, San Luis Potosí, Mexico. *Revista Mexicana de Ciencias Geológicas*, *41*(3), 206–220. doi.org/10.22201/igc.20072902e.2024.3.1828

Ferrusquia-Villafranca, I., Arroyo-Cabrales, J., Martinez-Hernandez, E., Gama-Castro, J., Ruiz-Gonzalez, J., Polaco, O. J., & Johnson, E. (2010). Pleistocene mammals of Mexico: A critical review of regional chronofaunas, climate change response and biogeographic provinciality. *Quaternary International*, *217*, 53–104. doi.org/10.1016/j.quaint.2009.11.036

Ferrusquía-Villafranca, I., Arroyo-Cabrales, J., Johnson, E., Ruiz-González, J., Martínez-Hernández, E., Gama-Castro, J., de Anda-Hurtado, P., & Polaco, O. J. (2017). Quaternary Mammals, People, and Climate Change: A View from Southern North America. In G. G. Monks, (ed.), *Climate Change and Human Responses: A Zooarchaeological Perspective*. Vertebrate Paleobiology and Paleoanthropology (27–67). New York, Springer. doi.org/10.1007/978-94-024-1106-5_3

Fish, J. (2004). Karst hydrology of the Sierra de El Abra, México. *Association for Mexican Cave Studies. Bulletin*, 14.

Flower, W. H. (1883). On the arrangement of the orders and families of existing Mammalia. *Proceedings of the Zoological Society of London*, 1883, 178–186.

Fricke, H. C., Rogers, R. R., Eberth, D. A., & Fiorillo, A. R. (2007). Stable isotope geochemistry of bonebed fossils: reconstructing paleoenvironments, paleoecology, and paleobiology. In *Bonebeds: genesis*, *analysis*, *and paleobiological significance* (pp. 437–490). University of Chicago Press Chicago. doi.org/10.7208/chicago/9780226723730.003.0008

Gervais, M. P. (1855). Recherches sur les mammifères fossiles de l'Amérique du Sud. In F., de Castelnau (Ed.), *Zoologie de l'Expédition dans les parties centrales de l'Amérique du Sud de Rio de Janeiro à Lima*, *et de Lima au Para* (pp. 1–63). Exécuté par ordre du Gouvernement français pendant les années 1843 à 1847 sous la direction du comte Francis de Castelnau.

Gillette, D. D., & Ray C. E. (1981). Glyptodonts of North America. *Smithsonian Contributions to Paleobiology*, *40*, 1–255. doi.org/10.5479/si.00810266.40.1

Godínez-Álvarez, H. (2004). Pollination and seed dispersal by lizards: a review. *Revista chilena de historia natural*, *77*(3), 569–577. doi.org/10.4067/s0716-078x2004000300015

Godínez-Alvarez, H., & Valiente-Banuet, A. (2000). Fruit-Feeding Behavior of the Bats *Leptonycteris curasoae* and *Choeronycteris mexicana* in Flight Cage Experiments: Consequences for Dispersal of Columnar Cactus Seeds1. *Biotropica*, *32*(3), 552–556. doi.org/10.1646/0006-3606(2000)032[0552:ffbotb]2.0.co;2

Godínez-Alvarez, H., Valiente-Banuet, A., & Rojas-Martínez, A. (2002). The role of seed dispersers in the population dynamics of the columnar cactus *Neobuxbaumia tetetzo*. *Ecology*, *83*(9), 2617–2629. doi.org/10.1890/0012-9658(2002)083[2617:trosdi]2.0.co;2

Gomes, V. G. N., Quirino, Z. G. M., & Araujo, H. F. P. (2014). Frugivory and seed dispersal by birds in *Cereus jamacaru* DC. ssp. *jamacaru* (Cactaceae) in the Caatinga of Northeastern Brazil. *Brazilian Journal of Biology*, *74*, 32–40. doi.org/10.1590/1519-6984.15312

Gomes, V. G. N., Meiado, M. V., Quirino, Z. G. M., & Machado, I. C. (2016). Seed removal by lizards and effect of gut passage on germination in a columnar cactus of the Caatinga, a tropical dry forest in Brazil. *Journal of Arid Environments*, *135*, 85–89. doi.org/10.1016/j.jaridenv.2016.08.013

Gray, J. E. (1821). On the natural arrangement of vertebrose animals. *The London Medical Repository*, 15, 296–310.

Hansen, R. M. (1978). Shasta ground sloth food habits, Rampart Cave, Arizona. *Paleobiology*, *4*, 302–319. doi.org/10.1017/s0094837300006011

Hoffstetter, R. (1954). Les gravigrades (Édentés, Xénarthres) des caverns de Lagoa Santa. *Annales des Sciences Naturelle*, *Zoologie* 11, 741–764.

Illiger, C. (1811). *Prodromus Systematics Mammalium et Avium Additis Terminis Zoographicis Utriusque Cassis*. Salfeld, Berlín, 301 p.

Jiménez Hidalgo, E., Pacheco Castro, A., Cruz, J. A., & Guerrero Arenas, R. (2024). Importancia, técnicas de recolecta y procesos curatoriales de pequeños vertebrados e invertebrados continentales fósiles. *Paleontología Mexicana*, *13*(2), 141–155. doi.org/10.22201/igl.05437652e.2024.13.2.383

Jiménez-Moreno, F. J., Morales-Tehuitzitl, E. D., Carbot-Chanona, G., & Velázquez-Castro, J. (2022). A mathematical model to calculate the population of *Mammuthus columbi* (Mammalia, Proboscidea, Elephantidae) during the Late Pleistocene in the Valsequillo Basin, Puebla, Mexico. *Historical Biology*, *34*(4), 750–758. doi.org/10.1080/08912963.2021.1946530

Keeling, C. D., Mook, W. G., & Tans, P. P. (1979). Recent trends in the 13C/12C ratio of atmospheric carbon dioxide. *Nature*, 277, 121–123. https://doi.org/10.1038/277121a0

Kingston, J. D., & Harrison, T. (2007). Isotopic dietary reconstructions of Pliocene herbivores at Laetoli: Implications for early hominin paleoecology. *Palaeogeography*, *Palaeoclimatology*, *Palaeoecology*, *243*(3-4), 272–306. doi.org/10.1016/j.palaeo.2006.08.002

Lucas, S. G. (2008). Pleistocene mammals from Yeroconte Honduras. In Neogene Mammals. Lucas, S.G. (ed.), *New Mexico Museum of Natural History and Science Bulletin*, *44*, 403–408.

Lucas, S. G. (2014). Late Pleistocene mammals from El Hatillo, Panama. *Revista geológica de América central*, *50*, 139–151. doi.org/10.15517/rgac.v0i50.15120

Lund, P. W. (1842). Blik paa Brasiliens Dyreverden før sidste Jordomvæltning. *Det Kongelige Danske Videnskabernes Selskabs Skrifter*, 9, 137–208.

Magoulick, K. M., Saupe, E. E., Farnsworth, A., Valdes, P. J., & Marshall, C. R. (2025). Evaluating migration hypotheses for the extinct *Glyptotherium* using ecological niche modeling. *Ecography*, p.e07499. doi.org/10.1111/ecog.07499

McDonald, H. G. (2002). Fossil Xenarthra of Mexico: A Review. In M. Montellano Ballesteros, & Arroyo J., Cabrales (eds.). *Avances en los estudios paleomastozoológicos en México* (pp. 227-248). Serie Arqueología, Instituto Nacional de Antropología e Historia.

McDonald, H. G. (2003). Sloth remains from North American caves and associated karst features. In B.W. Schubert, J.I. Mead & R.W. Graham (eds.). *Ice Age Cave Faunas of North America* (pp. 1-16). Indiana University Press and Denver Museum of Nature and Science.

McDonald, H. G. (2022). Paleoecology of the extinct Shasta ground sloth, *Nothrotheriops shastensis*, (Xenarthra, Nothrotheriidae): The physical environment. *Bulletin of the New Mexico Museum of Natural History and Science*, *88*, 33–43.

McDonald, H. G., & Jefferson. G.T. (2008). Distribution and habitat of *Nothrotheriops* (Xenarthra, Nothrotheridae) in the Pleistocene of North America. In X. Wang and L. G. Barnes (eds.), Geology and Vertebrate Paleontology of Western and Southern North America, Contributions in Honor of David P. Whistler. *Natural History Museum of Los Angeles County Science Series*, *41*, 313–331.

McDonald, H. G., Chatters, J. C., & Gaudin T. J. (2017). A new genus of megalonychid ground sloth (Mammalia, Xenarthra) from the late Pleistocene of Quintana Roo, Mexico. *Journal of Vertebrate Paleontology*, *37*(3), e1307206. doi.org/10.1080/02724634.2017.1307206

McDonald, H. G., Arroyo-Cabrales, J., Alarcón-Durán, I., & Espinosa-Martínez, D. V. (2020). First record of *Meizonyx salvadorensis* (Mammalia: Xenarthra: Pilosa) from the late Pleistocene of Mexico and its evolutionary implications. *Journal of Systematic Palaeontology*, *18*(22), 1829–1851. doi.org/10.1080/14772019.2020.1842816

Mitchell, R. W., Russell, W. H., & Elliot, W. R. (1977). *Mexican Eyeless Characin Fishes*, *Genus Astyanax: Environment*, *Distribution*, *and Evolution (12)*. The Museum, Texas Tech University Special Publications.

Mysterud, A., Langvatn, R., Yoccoz, N. G., & Chr, N. (2001). Plant phenology, migration and geographical variation in body weight of a large herbivore: the effect of a variable topography. *Journal of Animal Ecology*, *70*(6), 915–923. doi.org/10.1046/j.0021-8790.2001.00559.x

Oliveira, E. V., Porpino, K. O., & Barreto, A. L. M. F. (2010). On the presence of *Glyptotherium* in the Late Pleistocene of Northeasthern Brazil, and the status of '*Glyptodon*' and '*Chlamydotherium*' paleobiogeographic implications. *Neues Jahrbuch für Geologie und Paläontologie – Abhandlungen*, 258, 353–363. doi.org/10.1127/0077-7749/2010/0116

Omena, É. C., Silva, J. L. L. D., Sial, A. N., Cherkinsky, A., & Dantas, M. A. T. (2021). Late Pleistocene meso-megaherbivores from Brazilian Intertropical Region: isotopic diet ($\delta^{13}C$), niche differentiation, guilds and paleoenvironmental reconstruction ($\delta^{13}C$, $\delta^{18}O$). *Historical Biology*, *33*(10), 2299–2304. doi.org/10.1080/08912963.2020.1789977

Osborn, H. F. (1903). *Glyptotherium texanum*: A new glyptodont from the Lower Pleistocene of Texas. *Bulletin of the American Museum of Natural History*, *19*, 491–494.

Pérez-Crespo, V. A., Arroyo-Cabrales, J., Alva-Valdivia, L. M., Morales-Puente, P., & Cienfuegos-Alvarado, E. (2012). Diet and habitat definitions for Mexican glyptodonts from Cedral (San Luis Potosí, México) based on stable isotope analysis. *Geological Magazine*, *149*(1), 153–157. doi.org/10.1017/s0016756811000951

Pérez-Crespo, V. A., Carbot-Chanona, G., Morales-Puente, P., Cienfuegos-Alvarado, E., & Otero, F. J. (2015) Paleoambiente de la Depresión Central de Chiapas, con base en isótopos estables de carbono y oxígeno. *Revista Mexicana de Ciencias Geologicas*, *32*(2), 273–282.

Phillips, D. L. (2012). Converting isotope values to diet composition: the use of mixing models. *Journal of Mammology*, *93*(2), 342–352. doi.org/10.1644/11-mamm-s-158.1

Prevosti, F. J., & Vizcaíno, S. F. (2006). Paleoecology of the large carnivore guild from the Late Pleistocene of Argentina. *Acta Palaeontologica Polonica*, *51*(3), 407–422.

Ramírez-Cruz, G. A. & Montellano-Ballesteros, M. (2014). Two new glyptodont records (Mammalia: Cingulata) from the late Pleistocene of Tamaulipas and Tlaxcala, Mexico: implications for the taxonomy of the genus *Glyptotherium*. *The Southwestern Naturalist*, *59*(4), 522–530. doi.org/10.1894/jkf-45.1

Reimer, P. J., Bard, E., Bayliss, A., Beck, J. W., Blackwell, P. G., Ramsey, C. B., Buck, C. E., Cheng, H., Edwards, R. L., Friedrich, M. & Grootes, P. M. (2013). IntCal13 and Marine13 radiocarbon age calibration curves 0–50,000 years cal BP. *Radiocarbon*, 55(4), 1869-1887. doi.org/10.2458/azu_js_rc.55.16947

Reimer, P. J., Austin, W. E., Bard, E., Bayliss, A., Blackwell, P. G., Ramsey, C. B., Butzin, M., Cheng, H., Edwards, R. L., Friedrich, M., & Grootes, P.M. (2020). The IntCal20 Northern Hemisphere radiocarbon age calibration curve (0–55 cal kBP). *Radiocarbon*, *62*(4), 725–757. doi.org/10.1017/rdc.2020.41

Sagebiel, J. C. (2022). Xenarthrans from the Nueces River fauna, Upper Pleistocene of Nueces County, Texas. *New Mexico Museum of Natural History and Science Bulletin*, *88*, 225–232.

Sahagún-Sánchez, F. J., & De-Nova, J. A. (2020). Multi-taxonomic survey in the Sierra del Abra Tanchipa Biosphere Reserve. *Biota Neotropica*, *21*(1), e20201050.

Sánchez Salinas, M., Jiménez Hidalgo, E. & Castañeda Posadas, C. (2016). Mamíferos fósiles del Pleistoceno tardío (Rancholabreano) de San Mateo Huexoyucán, Tlaxcala, México. *Boletín de la Sociedad Geológica Mexicana*, *68*, 497–514. doi.org/10.18268/bsgm2016v68n3a7

Servicio Geológico Mexicano (2008). *Carta Geológico-Minera Álvaro Obregón F14-D11*, *Estado de San Luis Potosí* (Escala 1:50,000). Pachuca, Hidalgo, México: Secretaría de Economía.

Schubert, B. W., Chatters, J. C., Arroyo-Cabrales, J., Samuels, J. X., Soibelzon, L. H., Prevosti, F. J., Widga, C., Nava, A., Rissolo, D., & Erreguerena, P. L. (2019). Yucatán carnivorans shed light on the Great American Biotic Interchange. *Biology Letters*, *15*(5), 20190148. doi.org/10.1098/rsbl.2019.0148

Simpson, G. G. (1929). Pleistocene mammalian fauna of the Seminole Field, Pinellas County, Florida. *Bulletin of the American Museum of Natural History*, *56*, 561–599.

Sinclair, W. J. (1905). New mammalia from the Quaternary caves of California. University of California Publications, *Bulletin of the Department of Geological Sciences*, 4(7), 145–161.

Soibelzon, E., Zurita, A. E., & Carlini, A. A. (2006). *Glyptodon munizi* Ameghino (Mammalia, Cingulata, Glyptodontidae): redescripción y anatomía. *Ameghiniana*, *43*(2), 377e384.

Spillmann, F. (1948). Beiträge zur Kenntnis eines neuen gravigraden Riesensteppentieres (*Eremotherium carolinense* gen. et sp. nov.), seines Lebensraumes und seiner Lebensweise. *Palaeobiologica*, 8, 231–279.

Stinnesbeck, S. R., Frey, E., Olguín, J. A., Stinnesbeck, W., Zell, P., Mallison, H., González González, A., Aceves Núñez, E., Velázquez Morlet, A., Terrazas Mata, A. & Benavente Sanvicente, M. (2017). *Xibalbaonyx oviceps*, a new megalonychid ground sloth (Folivora, Xenarthra) from the Late Pleistocene of the Yucatán Peninsula, Mexico, and its paleobiogeographic significance. *PalZ*, 91, 245–271. doi.org/10.1007/s12542-017-0349-5

Tejada-Lara, J.V., MacFadden, B.J., Bermudez, L., Rojas, G., Salas-Gismondi, R., & Flynn, J.J. (2018). Body mass predicts isotope enrichment in herbivorous mammals. *Proceedings of the Royal Society B: Biological Sciences*, 285(1881), p.20181020. doi.org/10.1098/rspb.2018.1020

Valerio, A. L., Laurito, C.A., & Gomez, L. D. (2005). Un Gliptodonte (Xenarthra, Cingulata) de la Localidad de Chachagua, Provincia de Alajuela, Costa Rica. *Revista Geológica de America Central*, *32*, 61–63. doi.org/10.15517/rgac.v0i32.4245

Varela, L., Tambusso, P. S., McDonald, H. G., Vezzosi, R. I., & Fariña, R. A. (2023). Occurrence of the ground sloth *Nothrotheriops* (Xenarthra, Folivora) in the Late Pleistocene of Uruguay: new information on its dietary and habitat preferences based on stable isotope analysis. *Journal of Mammalian Evolution*, *30*, 561–576. doi.org/10.1007/s10914-023-09660-w

Vogel, J. S., Southon, J. R., Nelson, D. E., & Brown, T. A. (1984). Performance of catalytically condensed carbon for use in accelerator mass spectrometry. *Nuclear Instruments & Methods*, B5, 289–293. doi.org/10.1016/0168-583x(84)90529-9

Webb, S. D. (1978). A history of savanna vertebrates in the New World. Part II: South America and the Great Interchange. *Annual Review of Ecology and Systematics*, *9*, 393–426.

Webb, S. D., & Perrigo, S. C. (1984). Late Cenozoic vertebrates from Honduras and El Salvador. *Journal of Vertebrate Paleontology*, 4, 237–254. doi.org/10.1080/02724634.1984.10012006

Zurita, A. E., Carlini, A. A., Gillette, D., & Sánchez, R. (2011). Late Pliocene Glyptodontinae (Xenarthra, Cingulata, Glyptodontidae) of South and North America: morphology and paleobiogeographical implications in the GABI. *Journal of South American Earth Sciences*, *31*(2-3), 178–185. doi.org/10.1016/j.jsames.2011.02.001

Zurita, A. E., Gillette, D. D., Cuadrelli, F., & Carlini, A. A. (2018). A tale of two clades: comparative study of *Glyptodon* Owen and *Glyptotherium* Osborn (Xenarthra, Cingulata, Glyptodontidae). *Geobios*, *51*(3), 247–258. doi.org/10.1016/j.geobios.2018.04.004